

Electronic Supplementary Information (ESI)
for

**Revealing Internal Heavy Chalcogen Atom Effect on the Photophysics of
Dibenzo[*a,j*]phenazine-Cored Donor–Acceptor–Donor Triad**

*Shimpei Goto,^a Yuya Nitta,^a Nicolas Oliveira Decarli,^b Leonardo Evaristo de Sousa,^c Patrycja Stachelek,^d
Norimitsu Tohnai,^a Satoshi Minakata,^a Piotr de Silva,^{*c} Przemyslaw Data^{*be}, and Youhei Takeda^{*a}*

^a Department of Applied Chemistry, Graduate School of Engineering, Osaka University, Yamadaoka 2-1, Suita, Osaka 565-0871, Japan

^b Faculty of Chemistry, Silesian University of Technology, M. Strzody 9, 44-100 Gliwice, Poland

^c Department of Energy Conversion and Storage, Technical University of Denmark, Anker Engelunds Vej 301, 2800 Kongens Lyngby, Denmark

^d Durham University, Physics Department, South Road, Durham DH1 3LE, United Kingdom

^e Centre of Polymer and Carbon Materials, Polish Academy of Science, M. Curie-Sklodowskiej 34, 41-819, Zabrze, Poland

E-mail: pdes@dtu.dk; przemyslaw.data@polsl.pl; takeda@chem.eng.osaka-u.ac.jp

Table of Contents

General Remarks	S2
Synthetic Procedures and Spectroscopic Data of New Compounds	S3–S6
Single Crystal X-Ray Crystallographic Analysis	S7–S10
Steady-State UV-Vis Absorption and PL Spectra Measurement of PSeZ-DBPHZ-PSeZ and PTeZ-DBPHZ-PTeZ	S11
Theoretical Calculations	S12–S15
Powder X-ray Diffraction (PXRD) Analysis of PSeZ-DBPHZ-PSeZ	S16
Photoluminescence Response of the Ground Sample of PSeZ-DBPHZ-PSeZ against Solvent Vapor	S17
DSC Analysis of PSeZ-DBPHZ-PSeZ	S18
Photoluminescence Response of the As-Prepared PSeZ-DBPHZ-PSeZ against Acid/Base	S19
Steady-State Photoluminescence of PTeZ in Solid State and Zeonex [®] Film	S20
Time-Resolved Spectroscopy of Donors	S21
Fitting Lifetimes of D-A-D compounds and Donors	S22
Cyclic Voltammetry (CV)	S23
Thermogravimetric Analysis (TGA)	S24
OLED Fabrication and Characterization	S25
NMR Charts	S26–S32
References	S33–S34

General Remarks. All reactions were carried out under an atmosphere of nitrogen unless otherwise noted. Melting points were determined on a Stanford Research Systems MPA100 OptiMelt Automated Melting Point System. ^1H and ^{13}C NMR spectra were recorded on a JEOL JMTC-400/54/SS spectrometer (^1H NMR: 400 MHz, ^{13}C NMR: 100 MHz) using tetramethylsilane ($\delta = 0$ ppm) as an internal and external standard, respectively. $^{77}\text{Se}\{^1\text{H}\}$ NMR was recorded on a JEOL JMTC-400/54/SS spectrometer (76 MHz) using dimethylselenium ($\delta = 0$ ppm) as an external standard.^{S1} $^{125}\text{Te}\{^1\text{H}\}$ NMR was recorded on a JEOL JMTC-400/54/SS spectrometer (126 MHz) using diphenylditelluride ($\delta = 422$ ppm) as an external standard.^{S2} Infrared spectra were acquired on a SHIMADZU IRAffinity-1 FT-IR Spectrometer. Mass spectra (MS) and High-resolution mass spectra (HRMS) were obtained on a JEOL JMS-700 mass spectrometer. Steady-state UV-vis absorption and PL spectra of solutions were acquired on a Shimadzu UV-2550 UV-VIS spectrometer and HAMAMATSU C11347-01 spectrometer with an integrating sphere, respectively. Thermogravimetric analysis (TGA) was performed with TG/DTA-7200 system (SII Nano Technology Inc.). Differential scanning calorimetry (DSC) measurements were carried out on a DSC 6220 (SII) system at a scanning rate $10\text{ }^\circ\text{C min}^{-1}$ under a N_2 atmosphere. Powder X-ray diffraction (PXRD) patterns were recorded with a Rigaku SmartLab X-ray diffractometer with $\text{CuK}\alpha$ radiation ($\lambda = 1.5418\text{ \AA}$). Products were purified by chromatography on silica gel BW-300, Chromatorex NH (Fuji Silysia Chemical Ltd.), or NH-DM-1020. Analytical thin-layer chromatography (TLC) was performed on pre-coated silica gel glass plates (Wako silicagel 70 FM TLC plate and Fuji Silysia Chromatorex NH, 0.25 mm thickness). Compounds were visualized with UV lamp.

Materials. *tert*-Butyl bis(2-bromophenyl)carbamate (**S1**) [1453873-25-0] was prepared according to the procedure described in literature.^{S3} 3,11-Dibromo-dibenzo[*a,j*]phenazine (**Br2-DBPHZ**) [CAS No. 1620543-64-7] was prepared according to the procedure described in literature.^{S4} Commercial reagents were purchased from Sigma-Aldrich, TCI, or Wako Pure Chemical Industries, Ltd. and used as received. *t*-BuOH was dried over activated molecular sieves 3 \AA before use. Toluene and THF were purchased as dehydrated grade and purified by passing through a solvent purification system (KOREA KIYON Co., Ltd. and Nikko Hansen & Co., Ltd., respectively). Solvents of fluorescence spectroscopic grade were purchased from Nacalai Tesque Inc., Kanto Chemical Co., Inc. Wako Pure Chemical Industries for the measurement of UV-vis and emission spectra.

Theoretical Calculations. Molecular geometry optimizations were performed with density functional theory (DFT). Singlet and triplet excited state energies were calculated by means of time-dependent density functional theory in the Tamm-Dancoff (TDA) approximation^{S5} using the Gaussian 16 software.^{S6} The long-range corrected hybrid functional LC-wHPBE was used throughout along with the Def2-TZVP basis set. For each molecule, the range separation parameter (ω) of the functional was non-empirically tuned following the procedure outlined in reference.^{S7} For both D-A-D molecules, a ω value of 0.17 bohr^{-1} was found for all conformations. For the PSeZ and PTeZ donor fragments, ω values of 0.22 bohr^{-1} and 0.21 bohr^{-1} were found. Spin-orbit couplings were calculated with the QChem 5.1 software.^{S8} To properly take into account effects stemming from the medium in the excited state energies, a state-specific corrected linear response approach was employed^{S9} using toluene as the solvent. The energy decomposition analysis was done in the ADF at the PBE0/DZP level.

Electrochemistry. The electrochemical investigation was carried out using a Biologic SP150. The electrochemical cell comprised of the platinum electrode with a 1 mm diameter disc as a working electrode for electrochemical measurements and ITO glass as a working electrode for spectroelectrochemical one, Ag/AgCl electrode as a reference electrode and platinum coil as an auxiliary electrode. Cyclic voltamperometric measurements were conducted at room temperature at a scan rate of 50 mV/s and were calibrated against ferrocene/ferrocenium redox couple (unless stated otherwise).

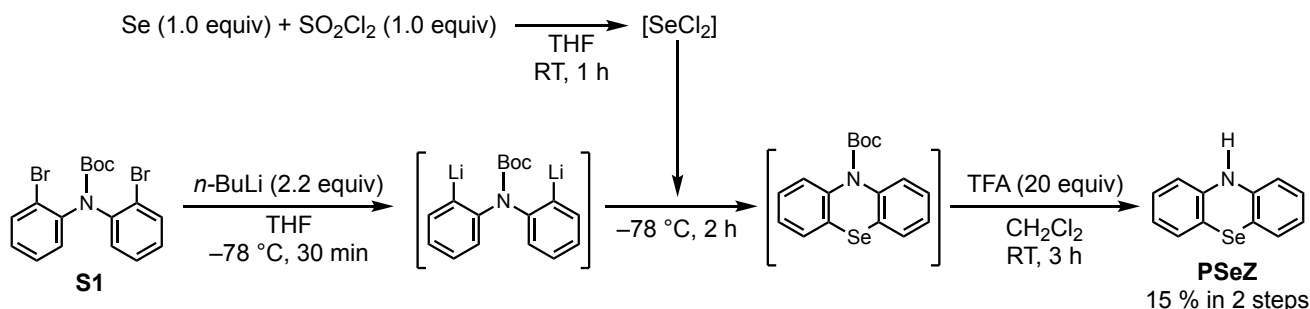
Photophysics. Phosphorescence, prompt fluorescence (PF), and delayed fluorescence (DF) spectra and fluorescence decay curves were recorded using nanosecond gated luminescence and lifetime measurements (from 400 ps to 1 s) using either third harmonics of a high energy pulsed DPSS laser emitting at 355 nm (Q-Spark-A50). Emission was focused onto a spectrograph and detected on a sensitive gated iCCD camera (Stanford Computer Optics) having sub-nanosecond resolution. Temperature photophysical measurements were conducted in Janis CCS-450 closed cycle helium cryostatic system.

OLED Devices. OLEDs have been fabricated on pre-cleaned, patterned indium-tin-oxide (ITO) coated glass substrates with a sheet resistance of $20\text{ }\Omega/\text{sq}$ and ITO thickness of 100 nm. All small molecules and cathode layers were thermally evaporated in Kurt J. Lesker Spectros 150 evaporation system under pressure of 10^{-7} mbar without breaking the vacuum. The sizes of the pixels were 4 mm^2 , 8 mm^2 and 16 mm^2 . All organic evaporated compounds were purified by CreaPhys organic sublimation system. All materials were purified by temperature-gradient sublimation in a vacuum. The characteristics of the devices were recorded using a 10-inch integrating sphere (Labsphere) connected to a Source Meter Unit and Ocean Optics USB4000 spectrometer.

Synthetic Procedures and Spectroscopic Data of New Comopounds.

Synthetic procedures of 3,11-Bis(10H-phenoselenazinyl)dibenzo[*a,j*]phenazine (PSeZ-DBPHZ-PSeZ)

Preparation of 10H-phenoselenazine (PSeZ) [CAS No. 262-05-5]



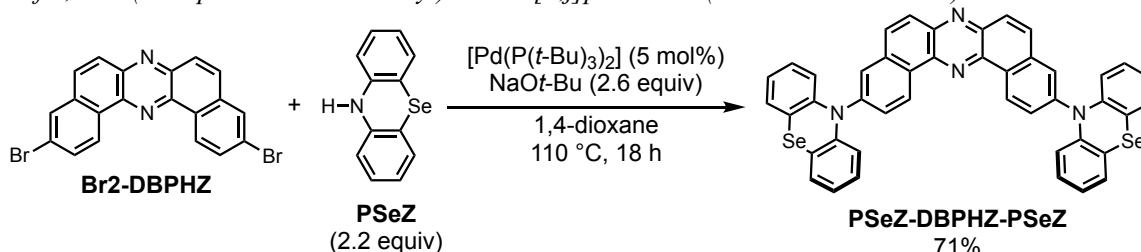
A three-necked round-bottomed flask (100 mL) equipped with a three-way cock, a septum, and a magnetic stirring bar was flame-dried and purged with N₂ gas. To the flask, were added *tert*-butyl bis(2-bromophenyl)carbamate (**S1**) (1.27 g, 3.0 mmol) and THF (9 mL) under a stream of N₂ gas, and the resulting solution was cooled to -78 °C. To the solution, a hexane solution of *n*-BuLi (1.6 M, 4.13 mL, 6.6 mmol) was added dropwise, and the resulting solution was stirred at -78 °C for 30 min (denoted as “*solution A*”).

Separately, SeCl₂ was prepared according to a slightly modified procedure in literature^[S10] as follows: separately, a two-necked flask (30 mL) equipped with a three-way cock, a septum, and a magnetic stirring bar was flame-dried and purged with N₂ gas. To the flask, were added Se powder (239.1 mg, 3.0 mmol), sulfuryl chloride (0.237 mL, 404.9 mg, 3.0 mmol), and the resulting mixture was stirred at room temperature for 10 min. THF (7.5 mL) was added to the flask, and the solution was stirred at room temperature for 1 h (denoted as “*solution B*”).

To the *solution A*, the *solution B* was added dropwise at -78 °C, and the resulting solution was stirred for 2 h. The reaction was quenched by adding water (20 mL), and the mixture was allowed warm up to room temperature. The resulting mixture was extracted with CH₂Cl₂ (30 mL × 3), and the combined organic extracts were dried over Na₂SO₄, filtered, and concentrated under vacuum to give the crude product (969. mg).

To a flask (50 mL) equipped with a magnetic stirring bar, was added the obtained crude product dissolved in dichloromethane (15 mL). To the solution, trifluoroacetic acid (4.4 mL, 57 mmol) was added dropwise, and the resulting mixture was stirred at room temperature for 3 h. The reaction was quenched with saturated NaHCO₃ aq. (15 mL). The organic layer was extracted with dichloromethane (30 mL × 3), and the combined organic layers were dried with Na₂SO₄, filtered, and concentrated under vacuum to give crude product (504.6 mg). The crude product was purified by flash column chromatography on NH silica gel (eluent: *n*-hexane/CH₂Cl₂ = 100:0 to 9:1) to afford **PSeZ** (209.4 mg), which was further purified by recrystallization from a biphasic solution of *n*-hexane/CH₂Cl₂ (2:1) to give pure **PSeZ** as yellow solids (111.0 mg, 15%). The spectroscopic data of **PSeZ** obtained by the method was in good agreement with those previously reported in literature.^{S11} mp 191.9 °C (dec); *R*_f 0.40 (*n*-hexane/AcOEt 8:2, NH silica); ¹H NMR (400 MHz, DMSO) δ 8.57 (brs, 1H), 7.09 (d, *J* = 8.4 Hz, 2H), 7.02 (dd, *J* = 7.6, 7.6 Hz, 2H), 6.78–6.74 (m, 4H); ¹³C NMR (100 MHz, CDCl₃) δ 142.1, 128.8, 127.7, 122.1, 115.1, 111.5; IR (ATR): ν 3383, 3046, 1593, 1566, 1458, 1439, 1302, 1275, 1260, 1234, 1130, 1115, 1061, 1026, 926, 856, 743, 716 cm⁻¹; MS (FAB⁺): *m/z* (relative intensity, %) 250 ([M+3]⁺, 5), 249 ([M+2]⁺, 17), 248 ([M+1]⁺, 26), 247 ([M]⁺, 84), 246 ([M-1]⁺, 17), 245 ([M-1]⁺, 43), 244 ([M-2]⁺, 20), 243 ([M-3]⁺, 17), 154 (100); HRMS (FAB⁺, NBA): *m/z* calcd for C₁₂H₉NSe (M) 246.9900, found 246.9904.

Synthesis of 3,11-di(10H-phenoselenazin-10-yl)dibenzo[*a,j*]phenazine (PSeZ-DBPHZ-PSeZ)

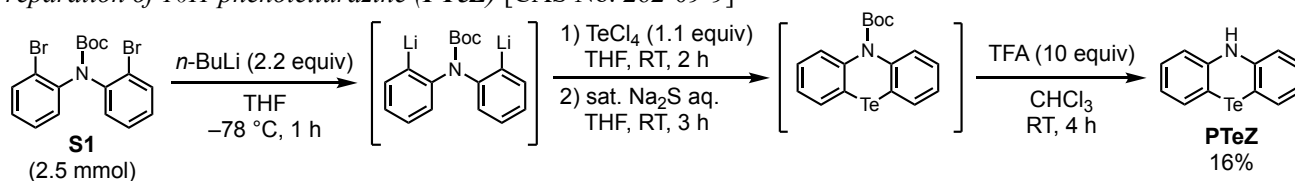


A two-necked reaction vessel (10 mL) equipped with a three-way-cock, a septum, and a stirring bar was flame-dried and purged with N₂ gas. To the vessel, were added dibromodibenzo[*a,j*]phenazine **Br2-DBPHZ** (43.8 mg, 0.10 mmol) and phenoselenazine **PSeZ** (54.2 mg, 0.22 mmol). The sealed vessel was transferred into a glovebox, where [Pd(P(*t*-Bu)₃)₂] (2.8 mg, 5.0 μmol, 5 mol%) and NaO*t*-Bu (25.0 mg, 0.26 mmol, 2.6 equiv) were added to the vessel. The flask was sealed with a rubber septum and transferred outside the glovebox. 1,4-dioxane (4.0 mL) was added to the flask. The mixture was stirred in a Personal Organic Synthesizer (EYELA, *Chemi-Station*) equipped with a cooling system under a reflux condition (110 °C) for 18 h. Water (6 mL) was added to the reaction mixture, and the organic layer was extracted

with CH₂Cl₂ (15 mL × 3). The combined organic extracts were dried over Na₂SO₄ and filtered, and the filtrate was concentrated under vacuum to give crude product (86.9 mg). The crude product was purified by flash column chromatography on NH silica gel (eluent: *n*-hexane/EtOAc 9:1) to give the product **PSeZ-DBPHZ-PSeZ** (71.4 mg), which were then further purified by recrystallization from a biphasic solution of *n*-hexane/CH₂Cl₂ (2:1) to afford pure **PSeZ-DBPHZ-PSeZ** as yellow solids (54.2 mg, 70.5 μmol, 71%). mp 325 °C (dec.); *R*_f 0.06–0.23 (observed as a broad spot, *n*-hexane/EtOAc 8:2, NH silica); *T*_d (5 wt%): 381 °C (under the air) *T*_d (5 wt%): 383 °C (under N₂); ¹H NMR (400 MHz, CDCl₃) δ 9.54 (dd, *J* = 8.4 Hz, 2H), 7.99 (d, *J* = 8.8 Hz, 2H), 7.88 (d, *J* = 9.2 Hz, 2H), 7.61–7.54 (m, 8H), 7.29–7.28 (m, 8H), 7.17–7.12 (m, 4H); ¹³C NMR (100 MHz, CDCl₃) δ 145.6, 142.6, 141.8, 140.7, 134.8, 131.8, 130.9, 127.7, 127.5, 126.8, 126.7, 126.6, 125.4, 125.0, 120.7, 117.2; ⁷⁷Se{¹H} NMR (76 MHz, CDCl₃) δ 317.7 (s); IR (ATR): ν 3057, 1605, 1584, 1570, 1543, 1476, 1462, 1435, 1352, 1315, 1302, 1277, 1254, 1148, 1123, 1032, 997, 972, 932, 854, 760, 748, 725 cm⁻¹; MS (EI): *m/z* (relative intensity, %): 772 ([M+2]⁺, 25), 771 ([M+1]⁺, 34), 770 (M⁺, 65), 768 ([M-2]⁺, 65), 766 ([M-4]⁺, 37), 611 ([M-2Se+1]⁺, 42), 610 ([M-2Se]⁺, 82), 444 (15), 305 (100), 166 ([Cbz]⁺, 21); HRMS (FAB⁺, NBA): *m/z* calcd for C₄₄H₂₆N₄Se₂ (M) 770.0488, found 770.0494; Anal. Cald for C₄₄H₂₆N₄Se₂: C, 68.75; H, 3.41; N, 7.29. found: C, 68.75; H, 3.75; N, 7.30.

Synthetic procedures of 3,11-Bis(10H-phenotelluraziny)dibenzo[*a,j*]phenazine (PTeZ-DBPHZ-PTeZ)

Preparation of 10H-phenotellurazine (PTeZ) [CAS No. 262-09-9]

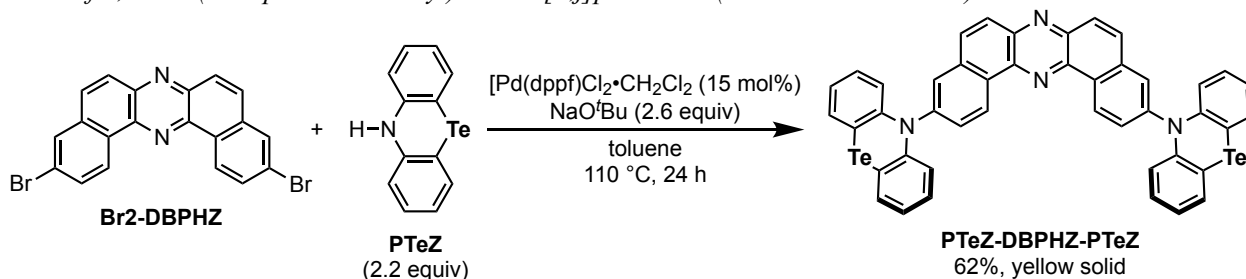


To a two-necked round-bottomed flask (100 mL) equipped with a magnetic stirring bar, was added *N*-Boc di(2-bromophenyl)amine (**S1**) (1.1 g, 2.5 mmol), and then the flask was sealed with rubber septums. The vessel was evacuated and replaced with N₂ gas for 3 times. THF (7.5 mL) was added to the flask through the septum, and the mixture was cooled to -78 °C. *n*-BuLi (hexane solution, 1.6 M, 3.4 mL, 5.5 mmol, 2.2 equiv) was added dropwise to the solution through the septum, and the resulting mixture was stirred for 30 min at -78 °C (*Solution A*). A THF solution of TeCl₄, which was prepared by dissolving 732.3 mg, (2.75 mmol, 1.1 equiv) of TeCl₄ in 14 mL of THF, was added dropwise to the *Solution A* through the septum at -78 °C. The resulting mixture was stirred at -78 °C for 5 min, and the mixture was allowed to warm up gradually to room temperature by removing the cooling bath and stirred for 2 h. Deionized water (20 mL) was added to the mixture, and the organic layer was extracted with CHCl₃ (25 mL × 3). The combined organic extracts were dried over Na₂SO₄ and filtered, and the solvents were evaporated in vacuo to give the yellow solid (1.16 g).

To a two-necked round-bottomed flask (50 mL) equipped with a magnetic stirring bar, were added the obtained yellow solid and THF (10 mL), and then the flask was sealed with rubber septums. The atmosphere in the flask was replaced with N₂ gas. Saturated Na₂S aq. (5 mL, 12 mmol; this corresponds to 4.8 equivalents against the theoretical maximum mole of cyclized Te(IV) intermediate, i.e., *tert*-butyl 5,5-dichloro-5λ⁴-phenotellurazine-10(5*H*)-carboxylate, which was calculated from the obtained weight) was added to the flask, and the resulting mixture was stirred at room temperature for 3 h. The organic layer was extracted with CHCl₃ (10 mL × 3), and the combined organic extracts were dried over Na₂SO₄ and filtered. The solvents were evaporated in vacuo to give orange oil (965.7 mg).

To a two-necked round-bottomed flask (50 mL) equipped with a magnetic stirring bar, were added a CHCl₃ solution of the obtained orange oil (15 mL), and then the flask was sealed with rubber septums. The atmosphere in the flask was replaced with N₂ gas. Trifluoroacetic acid (1.89 mL, 2.4 mmol; this corresponds to 10 equivalents against the theoretical maximum mole of *N*-Boc phenotellurazine calculated from the obtained weight) was added dropwise to the solution, and the resulting mixture was stirred at room temperature for 4 h. Saturated NaHCO₃ aq. (60 mL) was added to the mixture until the pH of the water layer became around 8 to quench the reaction, and the organic layer was extracted with CHCl₃ (10 mL × 3). The combined organic extracts were dried over Na₂SO₄ and filtered, and the solvent was evaporated in vacuo to give the crude product as dark orange viscous liquid (430.4 mg), which was purified by flash column chromatography on NH silica gel (eluent: *n*-hexane/ethyl acetate 9:1) followed by the precipitation from a two-phase solvent of *n*-hexane/CHCl₃ (1:6) to give **PTeZ** as yellow solid (116 mg, 0.39 mmol, 16 %). mp. 181 °C (dec.); *R*_f 0.30 (*n*-hexane/EtOAc 8:2 on NH silica gel TCL plate); ¹H NMR (400 MHz, CDCl₃) δ 7.37 (dd, *J* = 7.4, 1.4 Hz, 2H), 7.10 (ddd, *J* = 7.6, 7.6, 1.6 Hz, 2H), 6.86 (ddd, *J* = 7.4, 7.4, 1.2 Hz, 2H), 6.76 (dd, *J* = 7.8, 1.0 Hz, 2H), 6.17 (brs, 1H); ¹³C NMR (100 MHz, CDCl₃) δ 144.6, 135.1, 128.6, 123.8, 116.4, 97.9. Those spectroscopic data were in good agreement with those previously reported in literature.^{S12} IR (ATR, cm⁻¹): ν 3378, 3038, 1564, 1432, 1305, 1109, 1019, 851, 743; MS (EI) *m/z* (relative intensity, %): 297 (M⁺, 34), 295 ([M-2]⁺, 32), 293 ([M-4]⁺, 19), 167 ([M-Te]⁺, 100), 166 ([M-Te-H]⁺, 22); HRMS (EI): *m/z* calcd for C₁₂H₉NTe (M⁺) 296.9797, found 296.9800.

Synthesis of 3,11-Bis(10*H*-phenotellurazinyl)dibenzo[*a,j*]phenazine (**PTeZ-DBPHZ-PTeZ**)



To a two-necked reaction tube (10 mL) equipped with a magnetic stir bar, were added dibromodibenzo[*a,j*]phenazine **Br2-DBPHZ** (43.8 mg, 0.1 mmol), 10*H*-phenotellurazine **PTeZ** (76.8 mg, 0.22 mmol, 2.2 equiv), and Pd(dppf)Cl₂·CH₂Cl₂ (12.2 mg, 15 μmol, 15 mol%). The reaction tube was transferred into a glovebox, and NaO^t-Bu (25.0 mg, 0.26 mmol, 2.6 equiv) was added to the tube. The tube was sealed with rubber septums and transferred outside the glovebox. Toluene (5 mL) was added into the tube through the septum, and the resulting mixture was stirred in a Personal Organic Synthesizer (EYELA, *Chemi-Station*) equipped with a cooling system under a reflux condition (110 °C) for 24 h. Water (5 mL) was added to the reaction mixture, and the organic layer was extracted with CHCl₃ (10 mL × 3). The combined organic extracts were dried over Na₂SO₄ and filtered, and the solvents were evaporated in vacuo to give the crude product (97.9 mg) as a dark greenish viscous liquid, which was purified by gravity column chromatography on NH silica gel (eluent: *n*-hexane/ethyl acetate 8:2–6:4) followed by precipitation from a two-phase solvent of *n*-hexane/CH₂Cl₂ (3:1) to give **PTeZ-DBPHZ-PTeZ** as yellow solid (52.0 mg, 60%). *T*_d (5wt% loss) 412 °C (under N₂); 443 °C (air); mp 211 °C (dec.); *R*_f 0.04 (*n*-hexane/EtOAc 8:2 on NH silica gel TLC plate); ¹H NMR (400 MHz, CD₂Cl₂) δ 9.20 (d, *J* = 8.8 Hz, 2H), 7.95 (dd, *J* = 8.0, 1.6 Hz, 4H), 7.84 (9.6 Hz, 2H), 7.81 (dd, 8.0, 1.2 Hz, 4H), 7.71 (d, *J* = 9.2 Hz, 2H), 7.52 (ddd, *J* = 7.2, 7.2, 1.2 Hz, 4H), 7.23–7.27 (m, 6H), 7.17 (d, *J* = 2.8 Hz, 2H); ¹³C NMR (100 MHz, CDCl₃) δ 146.9, 143.7, 140.9, 137.4, 134.5, 131.4, 129.7, 128.8, 127.3, 127.0, 126.1, 123.9, 119.6, 114.7, 109.5 (1C is missing, probably due to the overlap of signals in the aromatic region); ¹²⁵Te NMR (400 MHz, CDCl₃) 408.6; IR (ATR, cm⁻¹): ν 2920, 1476, 1462, 1450, 1435, 1350, 1300, 1251, 1145, 744, 727, 715; MS (FAB⁺, NBA): *m/z* (relative intensity, %): 871 ([M+H]⁺, 6), 870 (M⁺, 6), 869 ([M–2+H]⁺, 10), 868 ([M–2]⁺, 6), 867 ([M–4+H]⁺, 10), 866 ([M–4]⁺, 7), 865 ([M–6+H]⁺, 8), 864 ([M–6]⁺, 5), 610 ([M–2Te]⁺, 4); HRMS (FAB⁺, NBA): *m/z* calcd for C₄₄H₂₇N₄Te₂ ([M–2+H]⁺) 869.0264, found 869.0360.

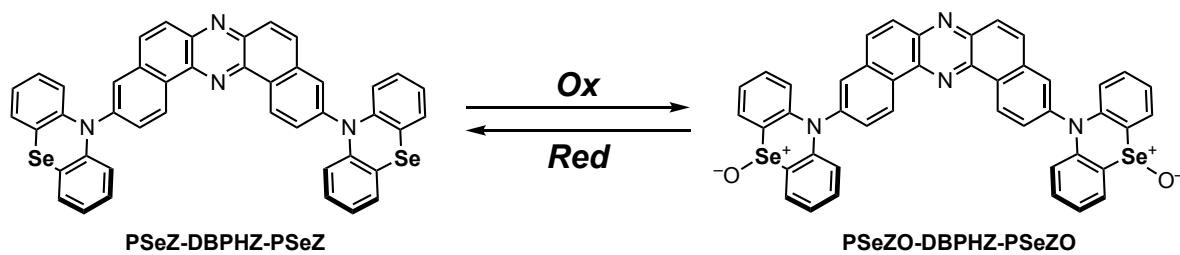
Oxidation/Reduction of PSeZ-DBPHZ-PSeZ/PSeZO-DBPHZ-PSeZO

Procedure for the oxidation of PSeZ-DBPHZ-PSeZ (Ox)

The oxidation of **PSeZ-DBPHZ-PSeZ** was conducted according to a method in literature.^[S13] To a two-necked reaction tube (10 mL) equipped with a magnetic stirring bar and septum, **PSeZ-DBPHZ-PSeZ** (10.3 mg, 13.4 μmol), MeOH (0.5 mL), and 1,2-dichloroethane (1.0 mL) were added. The resulting solution was cooled to 0 °C, and *N*-chlorosuccinimide (3.9 mg, 29.3 mmol, 2.2 equiv) was added to the solution, which was then stirred at 0 °C for 1 h. To the reaction mixture, sat. aq. NaHCO₃ (1.0 mL) was added at 0 °C, and the resulting mixture was stirred for 15 min. Water (1.0 mL) was added to the solution, and the solution was stirred for 15 min. The mixture was allowed to room temperature, and organic layer was extracted with CHCl₃ (15 mL × 2). The combined organic layer was dried over Na₂SO₄, filtered, and evaporated in vacuo to give **PSeZO-DBPHZ-PSeZO** as yellow solid (11.2 mg, quant). *R*_f 0.20 (chloroform only, NH silica); ¹H NMR (400 MHz, CDCl₃) δ 9.98 (d, *J* = 8.8 Hz, 2H), 8.27 (d, *J* = 8.8 Hz, 2H), 8.20 (d, *J* = 9.2 Hz, 2H), 8.15 (d, 2.0 Hz, 2H), 7.93–7.97 (m, 6H), 7.36 (ddd, *J* = 8.0 Hz, 8.0 Hz, 1.6 Hz, 4H) 7.21 (dd, *J* = 8.0 Hz, 8.0 Hz, 4H) 6.78 (d, *J* = 8.4 Hz, 4H); ¹³C NMR (100 MHz, CDCl₃) δ 143.5, 141.2, 140.3, 139.7, 135.6, 132.7, 132.3, 132.2, 131.5, 130.1, 130.0, 128.6, 128.5, 122.6, 120.9, 118.4; ⁷⁷Se{¹H} NMR (76 MHz, CDCl₃) δ 773.7 (s); MS (FAB⁺, NBA): *m/z* (relative intensity, %): 803 ([M+2]⁺, 2), 801 ([M]⁺, 2), 785 ([M–O]⁺, 5), 769 ([M–2O]⁺, 5), 611 ([M–(2Se=O)]⁺, 3); HRMS (FAB⁺, NBA): *m/z* calcd for C₄₄H₂₆N₄O₂Se₂ (M+1) 803.0386, found 803.0483.

Procedure for the reduction of PSeZO-DBPHZ-PSeZO (Red)

The reduction of **PSeZO-DBPHZ-PSeZO** was conducted according to a method in literature.^[S14] To a two-necked round-bottom flask (50 mL) equipped with a magnetic stirring bar and septum, **PSeZO-DBPHZ-PSeZO** (41.3 mg, 52.0 μmol) and 1,2-dichloroethane (6.0 mL) were added to solve the solid completely. To the solution, sat. aq. Na₂SO₃ (200 M, 2.0 mL, 0.40 mmol, 7.7 equiv) was added, and the resulting reaction mixture was stirred at room temperature for 24 h. The organic layer was extracted with CHCl₃ (10 mL × 3). The combined organic layer was dried over Na₂SO₄, filtered, and evaporated in vacuo to give **PSeZ-DBPHZ-PSeZ** as yellow solid (32.1 mg, quant).



conditions:

Ox

- 1) NCS (2.2 equiv)
1,2-dichloroethane/MeOH, 0 °C, 1 h
- 2) sat. NaHCO₃aq. (excess), 0 °C, 15 min
H₂O, 0 °C, 15 min

Red

- sat. Na₂SO₃aq. (excess)
- 1,2-dichloroethane, rt, 24 h

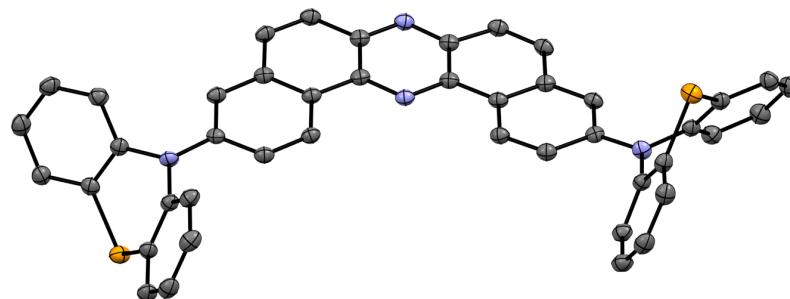
Single Crystal X-Ray Crystallographic Analysis.

Crystallographic analysis of polymorph **G**: The single crystal suitable for the X-ray crystallographic analysis was grown from a biphasic solution of *n*-hexane/CH₂Cl₂ (1:1 v/v) solution by slow evaporation. XtaLAB P200 diffractometer with graphite monochromated CuK α radiation ($\lambda = 1.54187 \text{ \AA}$) to a $2\theta_{\text{max}}$ value of 150.1° at 93 K. The cell refinements were performed with a software CrysAlisPro 1.171.39.5a.^{S15} The crystal structure was solved by direct methods (SHELXT Version 2014/5).^{S16} All calculations were performed with the observed reflections [$I > 2\sigma(I)$] with the program CrystalStructure crystallographic software packages,^{S17} except for refinement which was performed by SHELXL.^{S18} The non-hydrogen atoms were refined anisotropically, and hydrogen atoms were refined using the riding model. The crystal data are summarized in Table S1. Figure S1 shows packing structure of **G**. CCDC-2061434 contains the supplementary crystallographic data for **G**, which are available free of charge from the Cambridge Crystallographic Data Center (CCDC) via www.ccdc.cam.ac.uk/data_request/cif.

Crystallographic analysis of polymorph **Y**: The single crystal suitable for the X-ray crystallographic analysis was grown from a biphasic solution of *n*-hexane/CH₂Cl₂ (1:1 v/v) solution by slow evaporation. XtaLAB P200 diffractometer with graphite monochromated CuK α radiation ($\lambda = 1.54187 \text{ \AA}$) to a $2\theta_{\text{max}}$ value of 149.0° at 213 K. The cell refinements were performed with a software CrysAlisPro 1.171.39.5a.^{S15} The crystal structure was solved by direct methods (SHELXT Version 2014/5).^{S16} All calculations were performed with the observed reflections [$I > 2\sigma(I)$] with the program CrystalStructure crystallographic software packages,^{S17} except for refinement which was performed by SHELXL.^[S18] The non-hydrogen atoms were refined anisotropically, and hydrogen atoms were refined using the riding model. The crystal data are summarized in Table S2. Figure S2 shows packing structure of **Y**. CCDC-2061436 contains the supplementary crystallographic data for **Y**, which are available free of charge from the Cambridge Crystallographic Data Center (CCDC) via www.ccdc.cam.ac.uk/data_request/cif.

Crystallographic analysis of polymorph **O**: The single crystal suitable for the X-ray crystallographic analysis was grown from a biphasic solution of *n*-hexane/CH₂Cl₂ (1:1 v/v) solution by slow evaporation. XtaLAB P200 diffractometer with graphite monochromated CuK α radiation ($\lambda = 1.54187 \text{ \AA}$) to a $2\theta_{\text{max}}$ value of 149.0° at 93 K. The cell refinements were performed with a software CrysAlisPro 1.171.39.5a.^{S15} The crystal structure was solved by direct methods (SHELXT Version 2014/5).^{S16} All calculations were performed with the observed reflections [$I > 2\sigma(I)$] with the program CrystalStructure crystallographic software packages,^{S17} except for refinement which was performed by SHELXL.^{S18} The non-hydrogen atoms were refined anisotropically, and hydrogen atoms were refined using the riding model. The crystal data are summarized in Table S3. Figure S3 shows packing structure of **O**. CCDC-2061435 contains the supplementary crystallographic data for **O**, which are available free of charge from the Cambridge Crystallographic Data Center (CCDC) via www.ccdc.cam.ac.uk/data_request/cif.

Table S1. Summary of the crystallographic data of polymorph **G**.



Empirical Formula	C ₄₄ H ₂₆ N ₄ Se ₂ + solvent	
Formula Weight	768.64	
Crystal System	monoclinic	
Space Group	<i>I</i> 2/a (#15)	
Unit cell dimensions	<i>a</i> = 8.0558(2) Å	<i>α</i> = 90°
	<i>b</i> = 11.3915(3) Å	<i>β</i> = 94.548(3)°
	<i>c</i> = 37.9160(16) Å	<i>γ</i> = 90°
<i>V</i>	3468.51(19) Å ³	
<i>Z</i>	4	
Density (calculated)	1.472 g/cm ³	
Absorption coefficient	29.573 cm ⁻¹	
<i>R</i> ₁ [<i>I</i> > 2σ(<i>I</i>)]	0.0420	
<i>wR</i> ₂ (all data)	0.1248	
Crystal size	0.100 × 0.100 × 0.050 mm	
Goodness-of-fit on <i>F</i> ²	1.106	
Reflections collected/unique	18324/3501 [<i>R</i> (int) = 0.0442]	

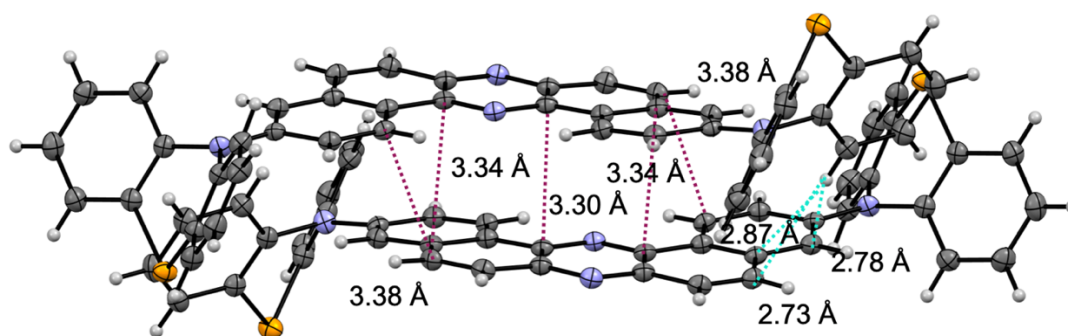
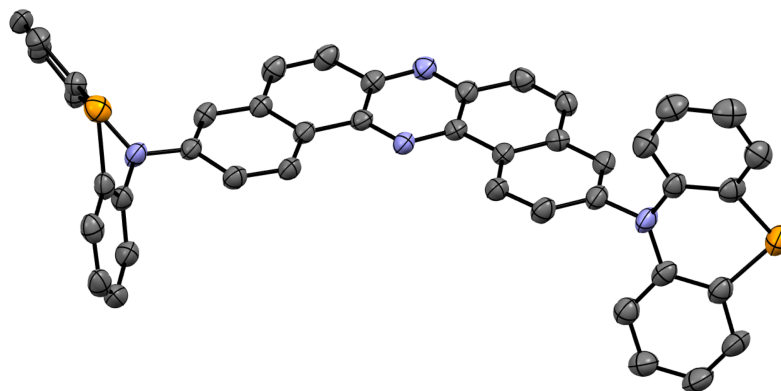


Fig. S1 Dimeric pair of PSeZ-DBPHZ-PSeZ in **G**.

Table S2. Summary of the crystallographic data of polymorph **Y**.



Empirical Formula	$C_{44}H_{26}N_4Se_2$
Formula Weight	768.64
Crystal System	monoclinic
Space Group	$P2_1/c$ (#14)
Unit cell dimensions	$a = 8.24949(17) \text{ \AA}$ $\alpha = 90^\circ$ $b = 17.3233(3) \text{ \AA}$ $\beta = 91.2052(19)^\circ$ $c = 22.8279(4) \text{ \AA}$ $\gamma = 90^\circ$
V	$3261.58(10) \text{ \AA}^3$
Z	4
Density (calculated)	1.565 g/cm^3
Absorption coefficient	31.449 cm^{-1}
R_1 [$I > 2\sigma(I)$]	0.0524
wR_2 (all data)	0.1472
Crystal size	$0.100 \times 0.010 \times 0.010 \text{ mm}$
Goodness-of-fit on F^2	0.990
Reflections collected/unique	20414/6449 [$R(\text{int}) = 0.0691$]

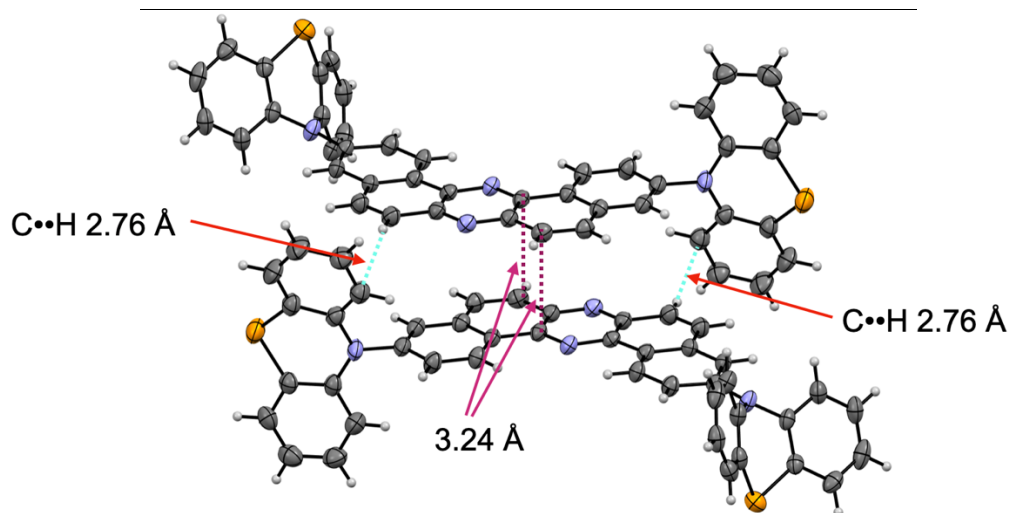
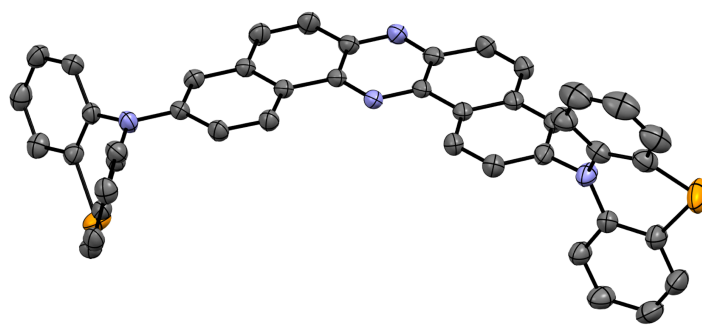


Fig. S2 Dimeric pair of PSeZ-DBPHZ-PSeZ in **Y**.

Table S3. Summary of the crystallographic data of polymorph **O**.



Empirical Formula	C ₄₄ H ₂₆ N ₄ Se ₂ + solvent	
Formula Weight	768.64	
Crystal System	monoclinic	
Space Group	C2/c (#15)	
Unit cell dimensions	$a = 30.3157(3) \text{ \AA}$	$\alpha = 90^\circ$
	$b = 8.60933(10) \text{ \AA}$	$\beta = 95.9262(11)^\circ$
	$c = 26.5579(3) \text{ \AA}$	$\gamma = 90^\circ$
V	6894.51(13) \AA^3	
Z	8	
Density (calculated)	1.481 g/cm ³	
Absorption coefficient	29.755 cm ⁻¹	
R_1 [$I > 2\sigma(I)$]	0.0418	
wR_2 (all data)	0.1178	
Crystal size	0.150 × 0.100 × 0.050 mm	
Goodness-of-fit on F^2	1.068	
Reflections collected/unique	20846/6866 [$R(\text{int}) = 0.0440$]	

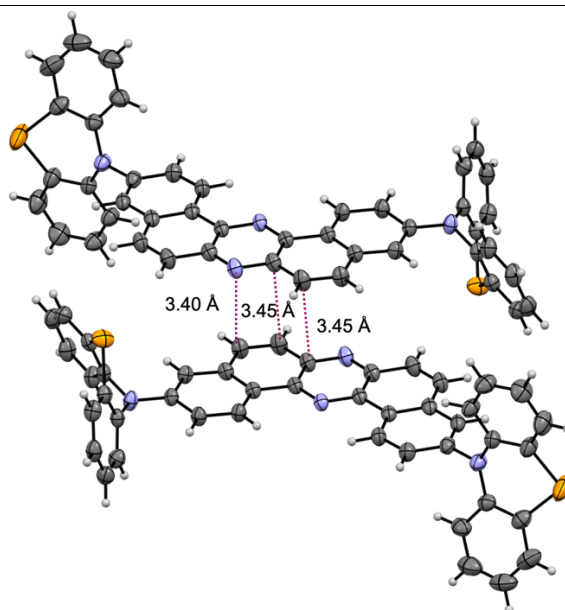


Fig. S3 Dimeric pair of PSeZ-DBPHZ-PSeZ in **O**.

Steady-State UV-Vis Absorption and PL Spectra Measurement of PSeZ-DBPHZ-PSeZ and PTeZ-DBPHZ-PTeZ.

For the measurement of solutions of PSeZ-DBPHZ-PSeZ and PTeZ-DBPHZ-PTeZ compounds, fluorescence spectroscopic grade solvents were purged with N₂ for 30 min before use. Steady-state UV-vis absorption and emission spectra were measured at room temperature using the solutions ($c = 1.0 \times 10^{-5}$ M). UV-vis spectra were recorded on a Shimadzu UV-2550 spectrophotometer. Steady-state emission spectra were recorded on a HAMAMATSU C11347-01 spectrometer with an integrating sphere. As for the measurements for solid samples, as-prepared solids, solids ground with mortar and pestle, and solids fumed with organic vapor were put in quartz petri dish with a lid, and PL spectra were acquired with HAMAMATSU C11347-01 spectrometer at room temperature under the ambient atmosphere.

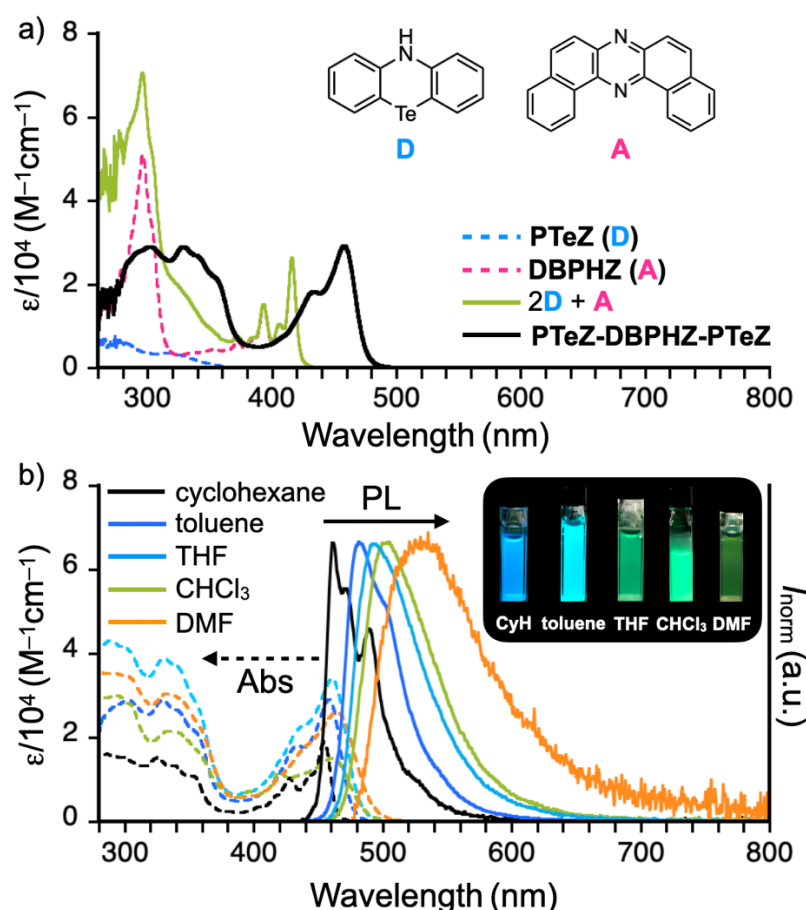


Fig. S4. a) UV-vis absorption spectra of PTeZ, DBPHZ, and PTeZ-DBPHZ-PTeZ in CH₂Cl₂ solution ($c = 10^{-5}$ M). b) UV-vis absorption and PL spectra of PTeZ-DBPHZ-PTeZ in various solvents ($c = 10^{-5}$ M, $\lambda_{\text{ex}} 365$ nm).

Table S4. Summary of steady-state photophysical properties of PTeZ-DBPHZ-PTeZ in solutions ($c = 10^{-5}$ M)

solvent	$\lambda_{\text{abs}}/\text{nm}$	$\epsilon/\text{M}^{-1}\text{cm}^{-1}$	$\lambda_{\text{em}}/\text{nm}$	Φ_{PL}^a
Cyclohexane	455	18,800	461	0.15
Toluene	458	29,200	481	0.14
THF	463	33,200	493	0.07
CHCl ₃	460	15,200	501	0.11
DMF	464	26,160	617	0.01

^aDetermined with an integrating sphere.

Theoretical Calculations.

Conformation Analysis

The probabilities assigned to the different conformations are calculated by means of a Boltzmann weighted average calculated at 300 K. The energies used to calculate the Boltzmann factors are taken from the equilibrium geometries for each conformation.

Table S5. Energies and probabilities associated with the different ground state conformations of **PSeZ-DBPHZ-PSeZ** in vacuum.

Conformation	Energy (eV)	Probability at 300 K
eq-eq	-182730.7656	0.07
eq-ax	-182730.8073	0.38
ax-ax	-182730.8162	0.55

Table S6. Energies and probabilities associated with the different ground state conformations of **PTeZ-DBPHZ-PTeZ** in vacuum.

Conformation	Energy (eV)	Probability at 300 K
eq-eq	-66620.48480	0.00
eq-ax	-66620.61222	0.02
ax-ax	-66620.71047	0.98

Table S7. Population probabilities at 300 K for **PSeZ-DBPHZ-PSeZ** conformers in different solvents.

Solvent/Conformation	eq-eq	eq-ax	ax-ax
Toluene	0.08	0.37	0.55
Cyclohexane	0.08	0.39	0.53
THF	0.06	0.31	0.63
Dichloromethane	0.06	0.30	0.64
Zeonex	0.08	0.38	0.54

Table S8. Energies and probabilities associated with the different ground state conformations of **PSeOZ-DBPHZ-PSeOZ** in toluene.

Conformation	Energy (eV)	Probability at 300 K
eq-eq	-6862.896994	0.48
eq-ax	-6862.896789	0.38
ax-ax	-6862.89587	0.14

Energy Decomposition Analysis

The total bonding energy of **PSeZ-DBPHZ-PSeZ** and **PTeZ-DBPHZ-PTeZ** with respect to the constituting atoms was decomposed into Pauli, electrostatic, orbital relaxation, and residual terms as implemented in the ADF program. The decomposition was done at the equilibrium geometries of both systems.

Table S9. Total bonding energy decomposition into Pauli, Electrostatic, Orbital relaxation, and Residual components. All energies in eV.

PSeZ-DBPHZ-PSeZ geometry										
	PSeZ-DBPHZ-PSeZ					PTeZ-DBPHZ-PTeZ				
	Total	Pauli	Electrost.	Orbital	Residual	Total	Pauli	Electrost.	Orbital	Residual
eq-eq	-633.21	2529.64	-505.18	-2657.61	-0.07	-629.08	2562.36	-518.28	-2673.10	-0.07
eq-ax	-633.27	2529.21	-505.06	-2657.35	-0.06	-629.28	2561.68	-518.08	-2672.81	-0.06
ax-ax	-633.28	2529.40	-504.98	-2657.64	-0.06	-629.43	2561.59	-517.90	-2673.06	-0.06
PTeZ-DBPHZ-PTeZ geometry										
	PSeZ-DBPHZ-PSeZ					PTeZ-DBPHZ-PTeZ				
	Total	Pauli	Electrost.	Orbital	Residual	Total	Pauli	Electrost.	Orbital	Residual

eq-eq	-631.90	2494.87	-494.30	-2632.40	-0.07	-630.94	2516.03	-502.68	-2644.23	-0.07
eq-ax	-631.97	2495.93	-494.48	-2633.36	-0.06	-631.12	2516.84	-502.76	-2645.13	-0.06
ax-ax	-632.00	2496.97	-494.62	-2634.28	-0.06	-631.26	2517.61	-502.81	-2646.00	-0.06

Excitation Energies

Table S10. Singlet and triplet excitation energies (eV) for **PSeZ-DBPHZ-PSeZ** conformers in toluene.

Conformation	eq-eq		eq-ax		ax-ax	
	Singlets	Triplets	Singlets	Triplets	Singlets	Triplets
1	2.9285	2.6119	2.9765	2.4425	3.0944	2.4704
2	3.0333	2.6765	3.0672	2.6475	3.1478	2.5747
3	3.0589	2.7138	3.0751	2.6946	3.3426	2.6847
4	3.3703	3.0133	3.4814	3.0676	3.6968	3.0186
5	3.3942	3.0172	3.5010	3.0960	3.7632	3.2038

Table S11. Singlet and triplet excitation energies (eV) for **PTeZ-DBPHZ-PTeZ** conformers in toluene.

Conformation	eq-eq		eq-ax		ax-ax	
	Singlets	Triplets	Singlets	Triplets	Singlets	Triplets
1	3.0750	2.6165	3.0716	2.4370	3.0928	2.4631
2	3.1697	2.6775	3.0786	2.6509	3.1496	2.5712
3	3.1886	2.7073	3.1128	2.6944	3.3405	2.6869
4	3.2017	2.8146	3.1956	2.7993	3.5087	3.0127
5	3.2028	2.8147	3.4915	3.0251	3.5089	3.0408

Absorption Spectra of PSeZ-DBPHZ-PSeZ and PTeZ-DBPHZ-PTeZ

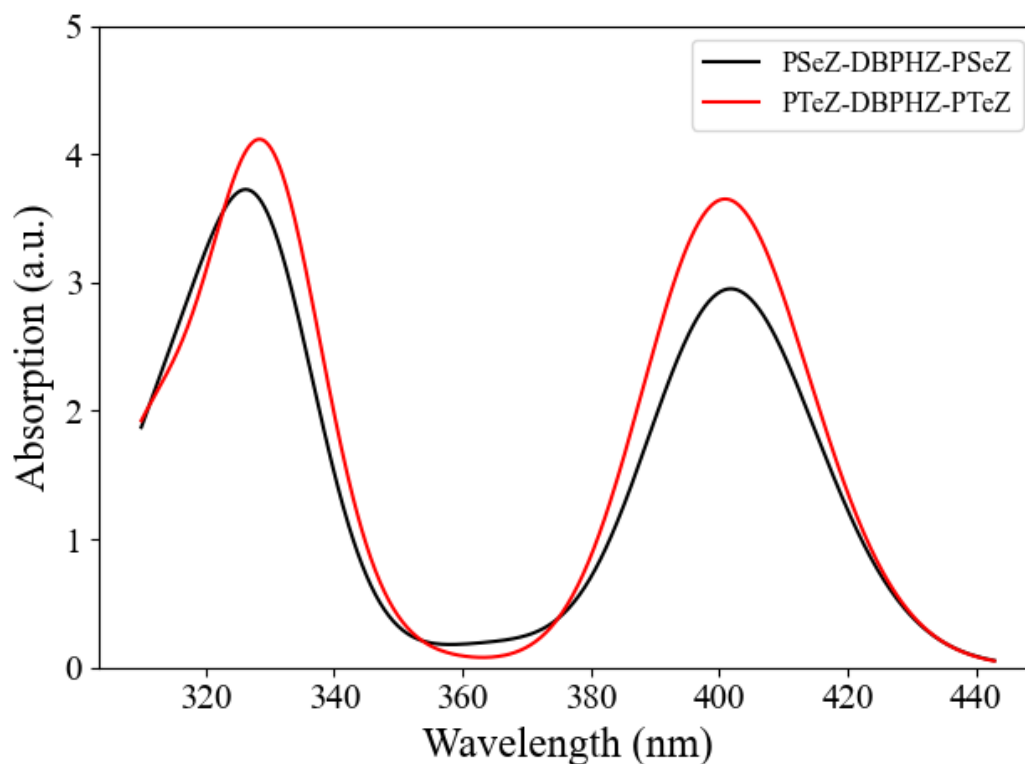


Fig. S5 Absorption spectra of **PSeZ-DBPHZ-PSeZ** and **PTeZ-DBPHZ-PTeZ** in toluene. The spectra are weighted according to the expected population of each of the three conformations at 300 K. A total of 10 excited states were taken into account, and transitions were broadened by gaussian functions with a standard deviation of 0.1 eV.

S₁ Geometries of PSeZ-DBPHZ-PSeZ



Fig. S6 eq-eq and eq-ax S₁ geometries for PSeZ-DBPHZ-PSe

Emission Energies of PSeZ-DBPHZ-PSeZ and PTeZ-DBPHZ-PTeZ

Table S12. Lowest singlet excited state energies calculated at corresponding excited state geometries.

Molecules	PSeZ- DBPHZ- PSeZ		PTeZ-DBPHZ-PTeZ	
	Toluene	THF	Toluene	THF
Conformation/Solvent				
eq-eq	2.04	1.72	2.07	1.74
eq-ax	2.22	1.89	2.81	2.73
ax-ax	2.52	2.54	2.53	2.54

Table S13. Lowest triplet excited state energies calculated at corresponding excited state geometries.

Molecules	PSeZ- DBPHZ- PSeZ		PTeZ-DBPHZ-PTeZ	
	Toluene	THF	Toluene	THF
Conformation/Solvent				
eq-eq	2.09	2.07	1.90	1.91
eq-ax	2.00	1.96	2.00	1.95
ax-ax	2.03	1.99	2.03	1.99

Emission Energies, SOCs, NTOs and Oscillator Strengths for Donor PSeZ and PTeZ

Table S14. Spin-orbit couplings, emission energies and oscillator strengths for PSeZ and PTeZ.

	PSeZ	PTeZ
Emission S_1 (eV)	2.96	2.35
Emission T_1 (eV)	2.33	1.87
$\langle S_0 H_{\text{soc}} T_1 \rangle$ (cm^{-1})	150.62	13.51
$\langle S_1 H_{\text{soc}} T_1 \rangle$ (cm^{-1})	3.00	0.00
Osc. Str. S_1	0.018	0.00

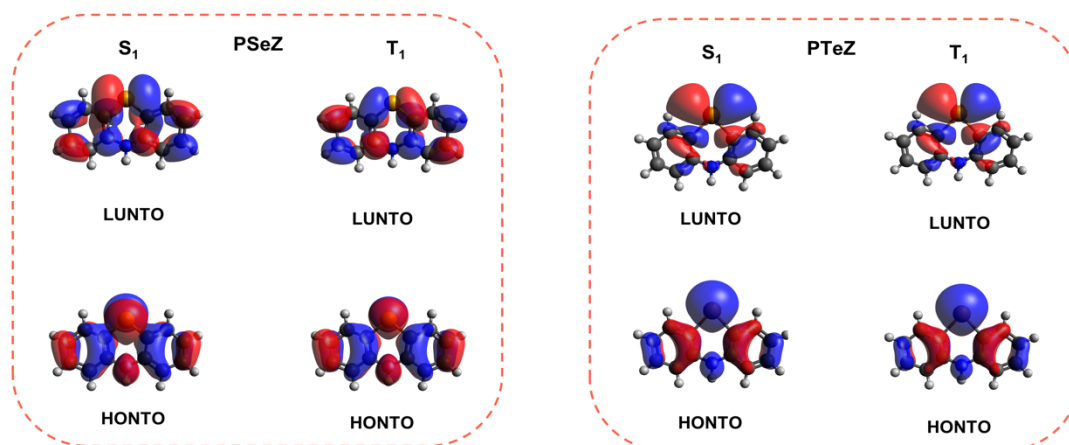


Fig. S7 NTOs for the PSeZ and PTeZ donor fragments.

NTOs for T_2 and T_3

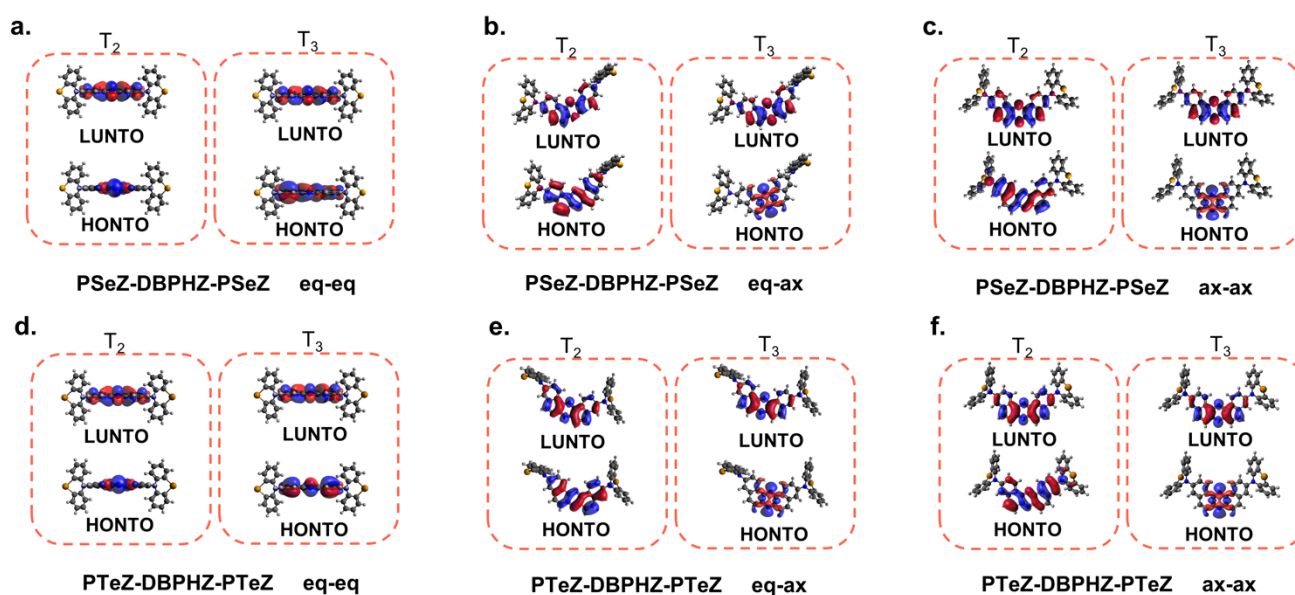


Fig. S8 NTOs for T_2 and T_3 states of the different conformations of a)–c) PSeZ-DBPHZ-PSeZ and d)–f) PTeZ-DBPHZ-PTeZ.

Powder X-ray Diffraction (PXRD) Analysis of PSeZ-DBPHZ-PSeZ.

Powder X-ray diffraction (PXRD) data were collected on a Rigaku Ultima IV instrument (40 kV, 40 mA) using graphite-monochromated CuK α radiation ($\lambda = 1.54187 \text{ \AA}$) at room temperature. The scan rate was $2.0^\circ \text{ min}^{-1}$.

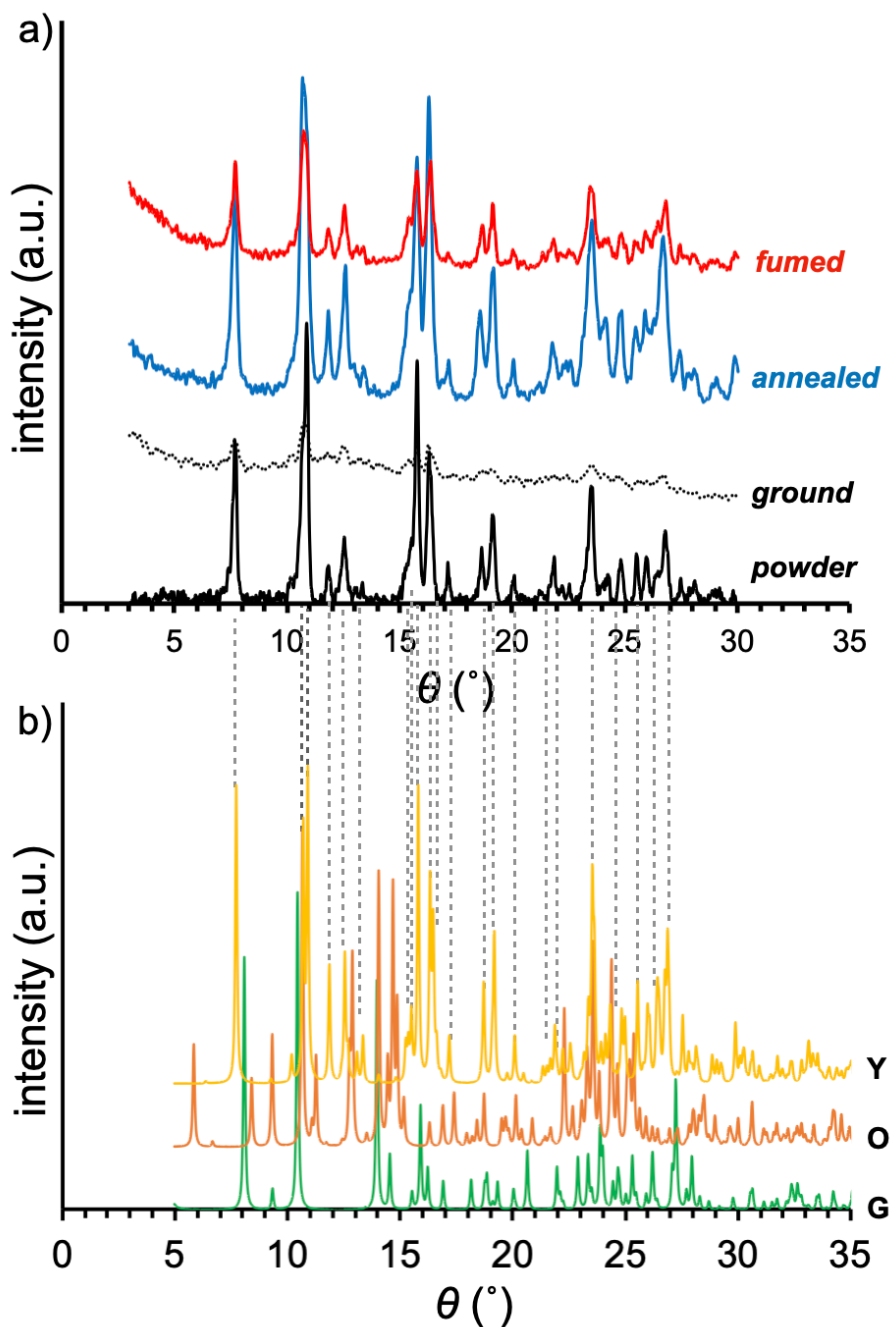


Fig. S9 PXRD spectra of a) powder (black solid line), ground (black dotted line), annealed (blue solid line), and fumed with DCM vapor (red solid line) samples of PSeZ-DBPHZ-PSeZ: b) PXRD patterns predicted from the polymorphs G (green), O (orange), and Y (yellow).

Photoluminescence Response of the Ground Sample of PSeZ-DBPHZ-PSeZ against Solvent Vapor.

The **powder** sample was prepared from reprecipitation from *n*-hexane/ CHCl_3 followed by dry under vacuum as yellow powdery solids. The **powder** was ground by mortar and pestle for 20 min to give **ground** sample. The **heat** sample was obtained by heating **ground** sample on a hotplate set at 220 °C for 15 min. Solids fumed with organic solvent (**DCM**, **AcOEt**, **CHCl_3** , and ***n*-hexane**) were obtained by fuming **powder** sample with the corresponding organic vapor inside double-layered vial systems for the indicated time in the Figure, where the inner and smaller vial that contains **powder** solid was soaked into the organic solvent in the outer and larger vial.

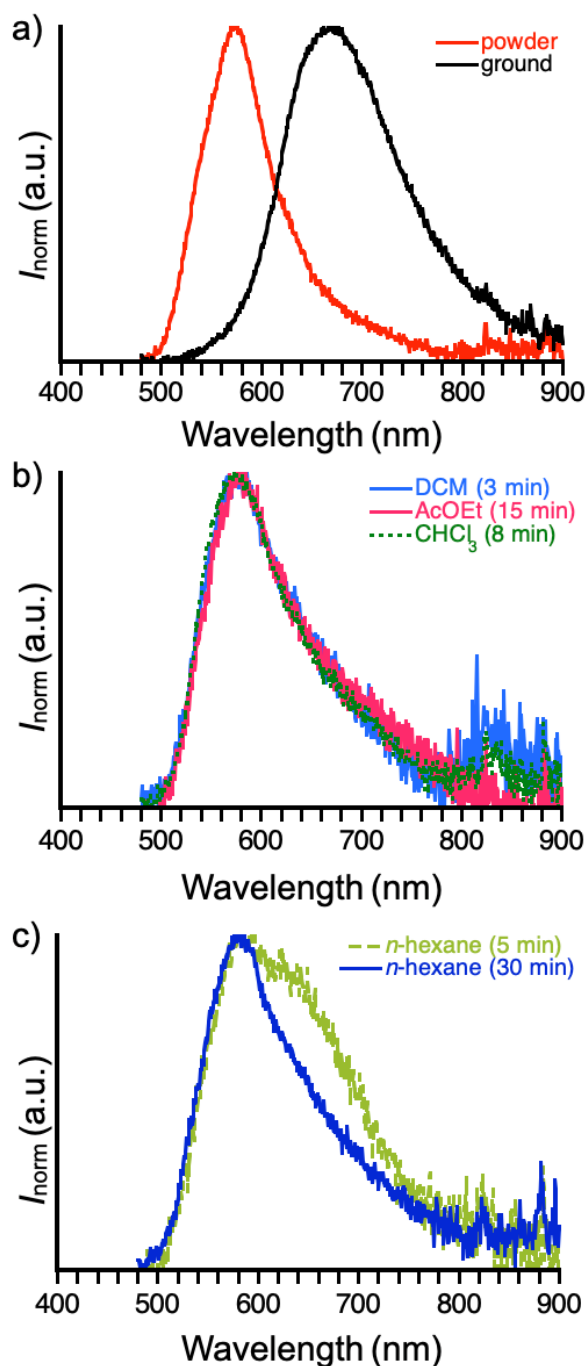


Fig. S10 PL spectra of (a) powder and ground solids, (b) solid samples fumed with DCM, AcOEt, and CHCl_3 vapor, and (c) solid samples fumed with *n*-hexane (λ_{ex} 400 nm).

DSC Analysis of PSeZ-DBPHZ-PSeZ.

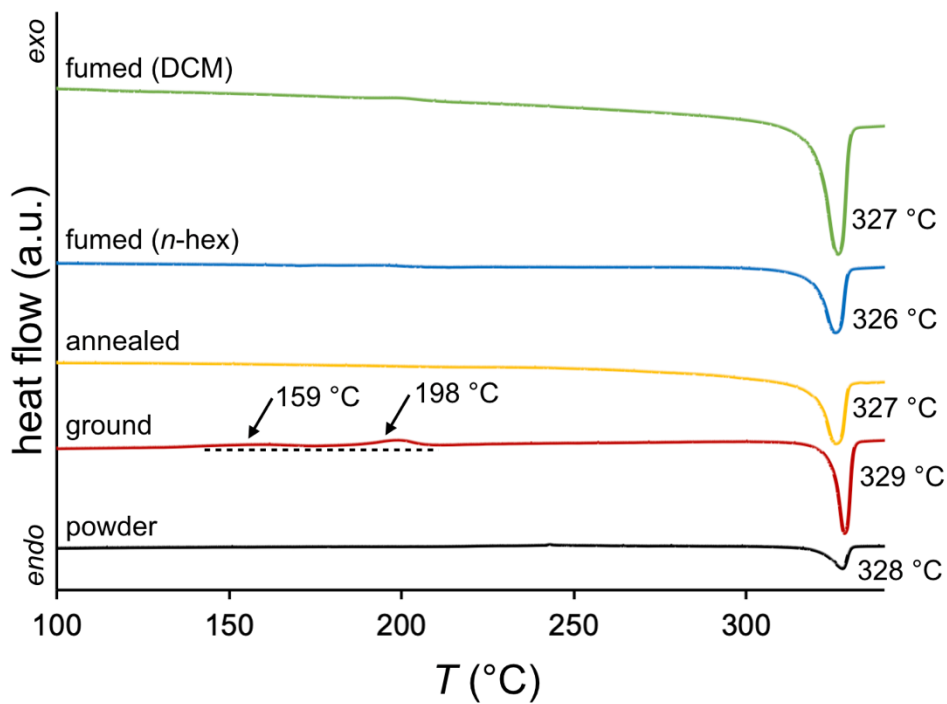


Fig. S11 DSC curves of the solids (powder: black line, ground: red line, annealed: orange line, fumed (n-hex): blue line, and fumed (DCM): green line).

Photoluminescence Response of the As-Prepared PSeZ-DBPHZ-PSeZ against Acid/Base.

To investigate the response of photoluminescence (PL) properties of **PSeZ-DBPHZ-PSeZ** against acid and base, **powder** solid was fumed with trifluoroacetic acid (TFA) for 3 min. This quenches the PL of **powder** (dark grey solid line in Figure S9 a). The PL was recovered by treating the resultant solid with triethylamine (TEA) vapor for 30 min with a slight broadened PL spectra (sky blue line in Figure S8a). This acid/base response was reproducible by repeating the cycle (green line in Figure S8a).

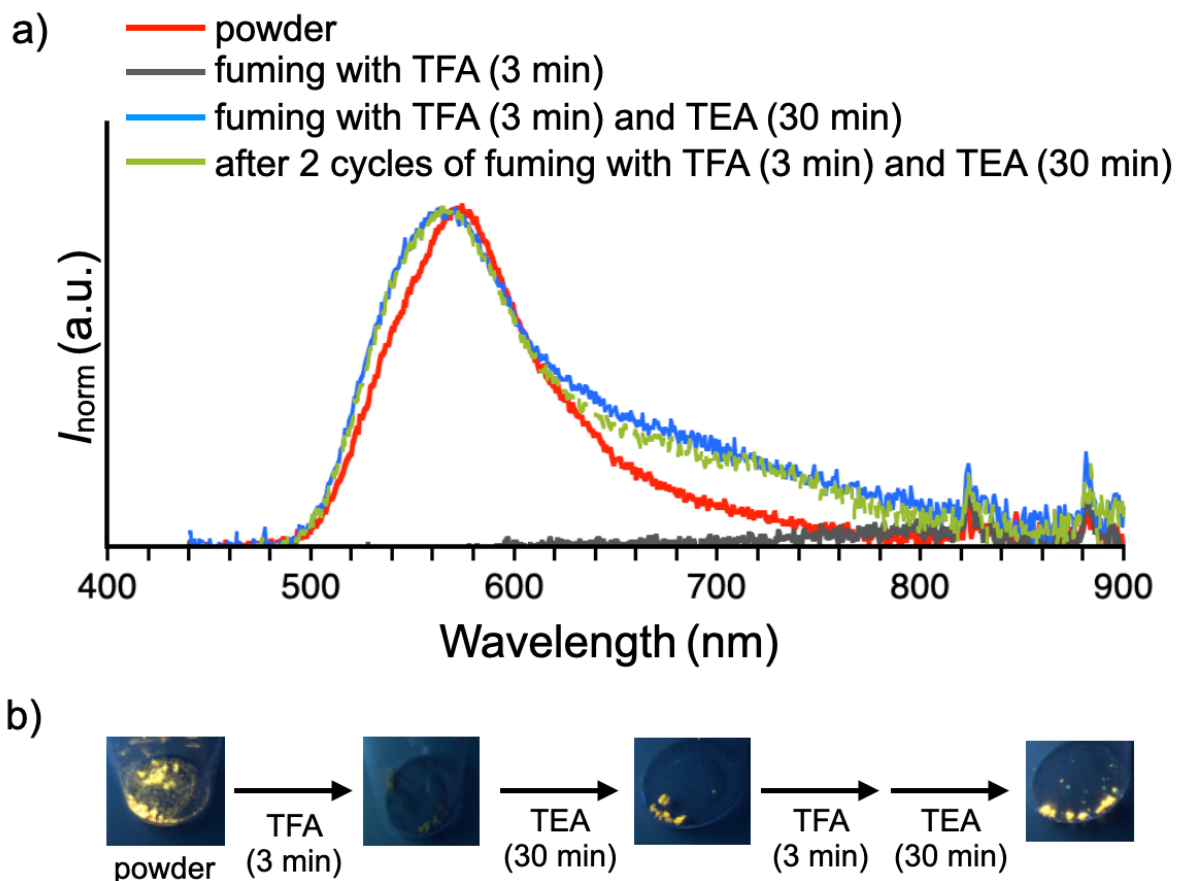


Fig. S12 a) PL spectra of samples treated with acid and base vapor (λ_{ex} 400 nm); b) Photographs taken under a UV lamp (λ 365 nm) in the acid/base fuming cycle.

Steady-State Photoluminescence of PTeZ in Solid State and Zeonex® Film

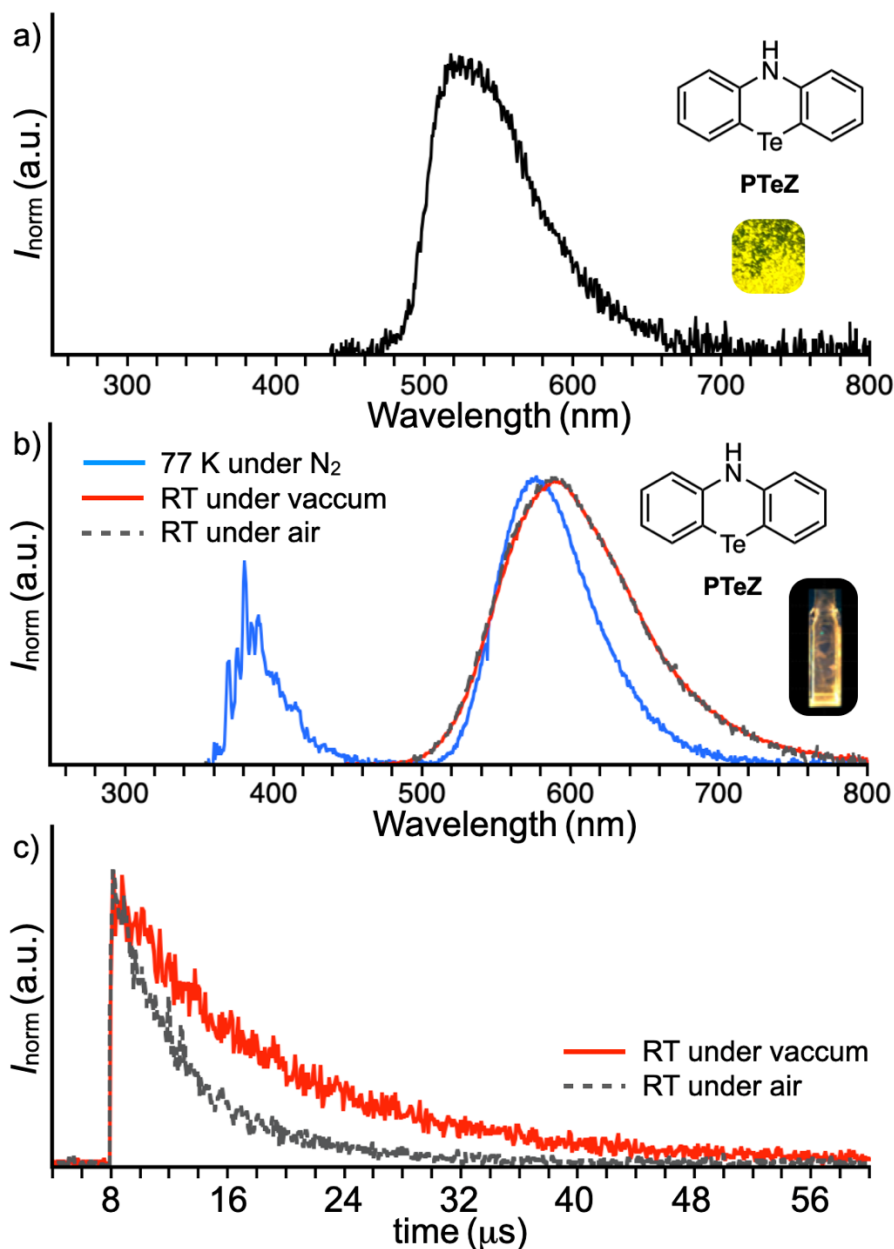


Fig. S13 a) PL spectrum of PTeZ in a) the solid state (λ_{ex} 330 nm); b) PL spectra of PTeZ in Zeonex® at 77 K under N₂ (sky-blue solid line), at room temperature under vacuum (red solid line), and at room temperature under air (grey dotted line); the inset photograph of the film under vacuum is taken under the irradiation of a UV lamp (λ 365 nm) (λ_{ex} 330 nm); c) Time decay of the PL (λ_{em} 591 nm; λ_{ex} 330 nm) in the Zeonex® at room temperature under vacuum (red solid line) and at room temperature under air (grey dotted line).

Time-Resolved Spectroscopy of Donors.

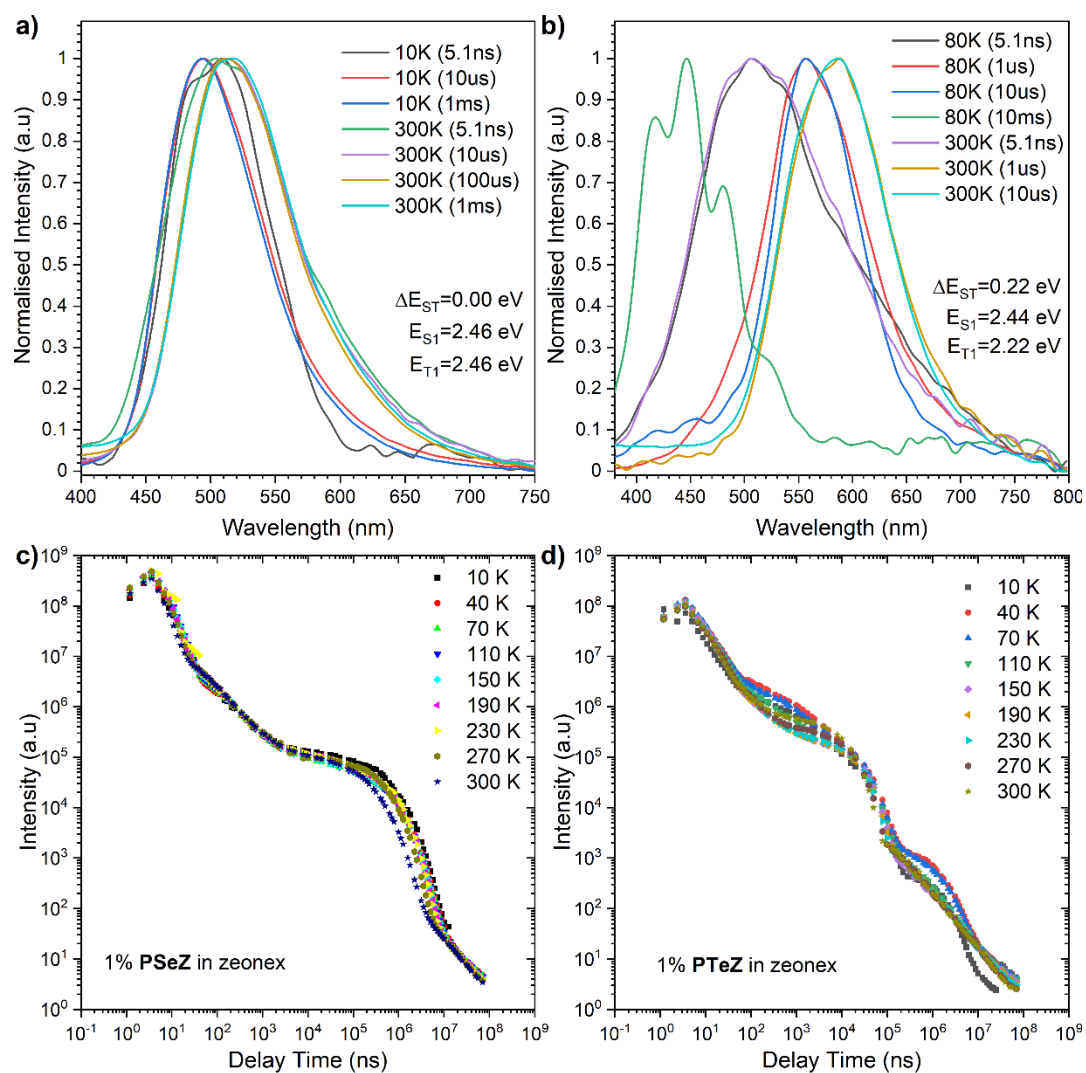


Fig. S14 Time-resolved spectra of 1% a) PSeZ and b) PTeZ in Zeonex[®]. Photoluminescence decay of respective samples c) PSeZ and d) PTeZ at different temperatures.

Fitting Lifetimes of D-A-D compounds and Donors

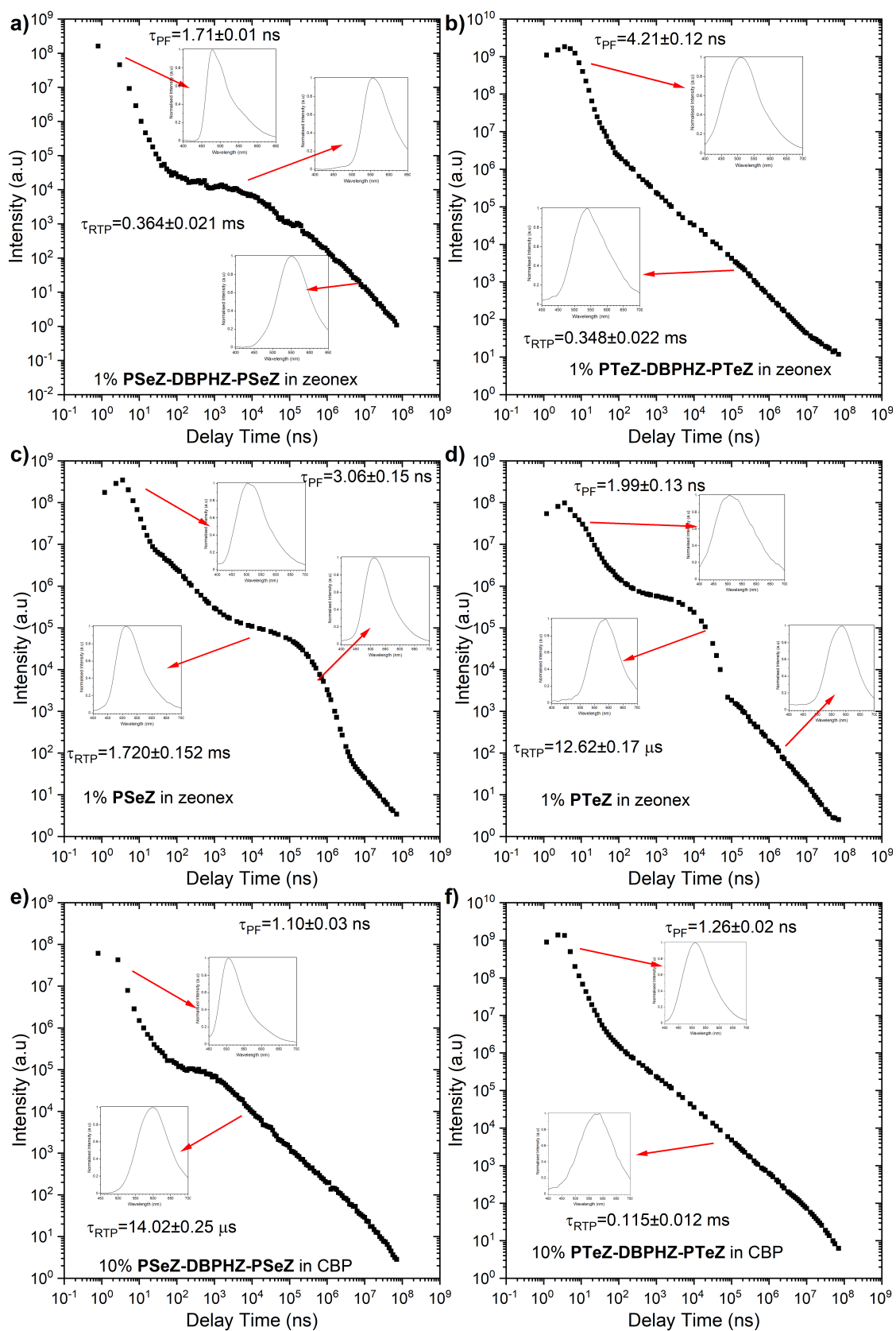


Fig. S15 Fitting lifetimes of the time-resolved spectroscopic data of (a) 1% PSeZ-DBPHZ-PSeZ in Zeonex[®], (b) 1% PTeZ-DBPHZ-PTeZ in Zeonex[®], (c) 1% PSeZ in Zeonex[®], (d) 1% PTeZ in Zeonex[®], (e) 10% PSeZ-DBPHZ-PSeZ in CBP, and (f) 10% PTeZ-DBPHZ-PTeZ in CBP.

Cyclic Voltammetry (CV).

The compounds of **PSeZ-DBPHZ-PSeZ** (10^{-3} M), **PTeZ-DBPHZ-PTeZ** ($\sim 10^{-3}$ M), **PSeZ** (10^{-3} M) and **PTeZ** ($\sim 10^{-3}$ M) were prepared and analysed in 0.1M $t\text{Bu}_4\text{N}^+\text{BF}_4^-$ dichlorometane electrolyte. Analysis were conducted at room temperature inside the glovebox in a cell equipped with a Pt disc as the working electrode (scanning rate: 50 mV/s). A Pt and Ag wires were applied as the counter and the reference electrode, respectively. The IP/EA and HOMO/LUMO energy levels were calculated by the following equation using the onset potentials corrected against the Fc/Fc^+ (Fc = ferrocene) redox couple: $\text{IP} = -\text{HOMO} = 5.1 + {}^{\text{ox}}E_{\text{onset}}/\text{V}$ [eV]; $\text{EA} = -\text{LUMO} = 5.1 + {}^{\text{red}}E_{\text{onset}}/\text{V}$ [eV].^{S19}

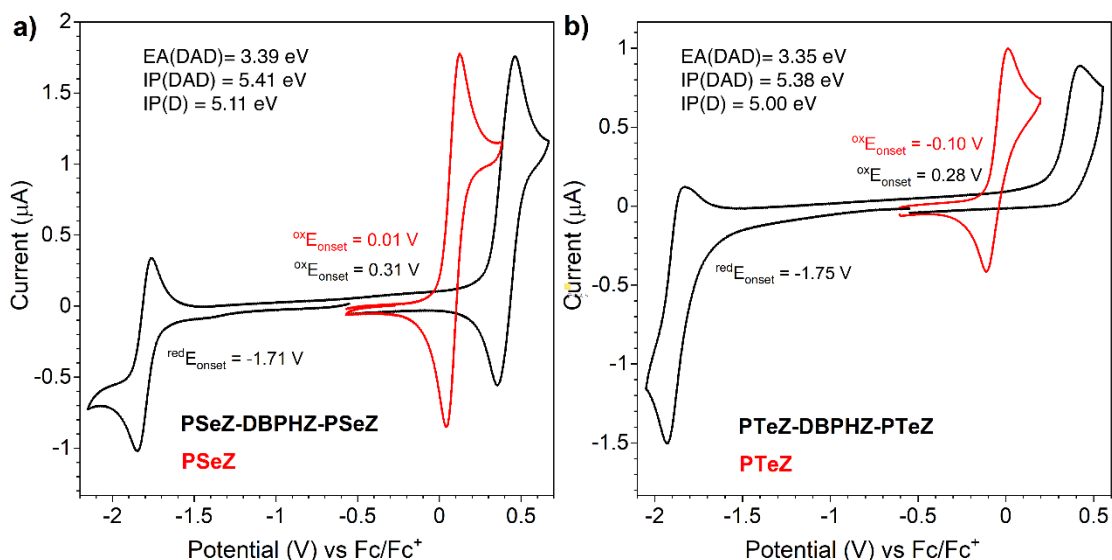


Fig. S16 Cyclic voltamperometric analysis of (a) **PSeZ-DBPHZ-PSeZ** and **PSeZ** in 0.1 M $t\text{Bu}_4\text{N}^+\text{BF}_4^-$ dichlorometane electrolyte, (b) **PTeZ-DBPHZ-PTeZ**, and **PTeZ** in 0.1M $t\text{Bu}_4\text{N}^+\text{BF}_4^-$ dichlorometane electrolyte

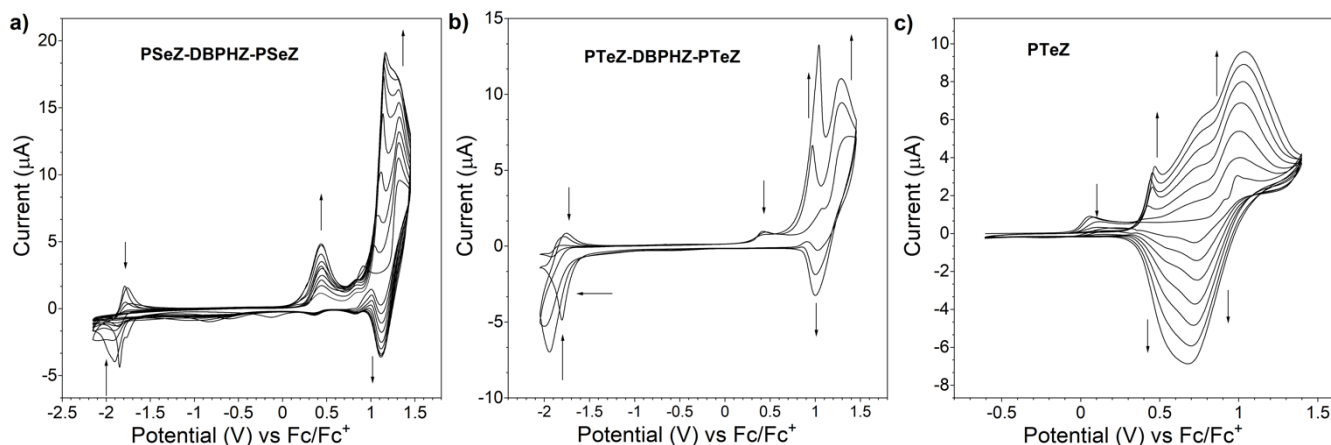


Fig. S17 Cyclic voltamperometric analysis of electropolymerisation processes of (a) **PSeZ-DBPHZ-PSeZ**, (b) **PTeZ-DBPHZ-PTeZ**, and (c) **PTeZ** in 0.1M $t\text{Bu}_4\text{N}^+\text{BF}_4^-$ dichlorometane electrolyte

Thermogravimetric Analysis (TGA).

The TGA profiles of **PSeZ-DBPHZ-PSeZ** and **PTeZ-DBPHZ-PTeZ** were obtained using a Pt pan under the air or the N₂ gas flow (200 mL/min), starting from 40 °C to 1000 °C at the ramp rate of 10 °C/min.

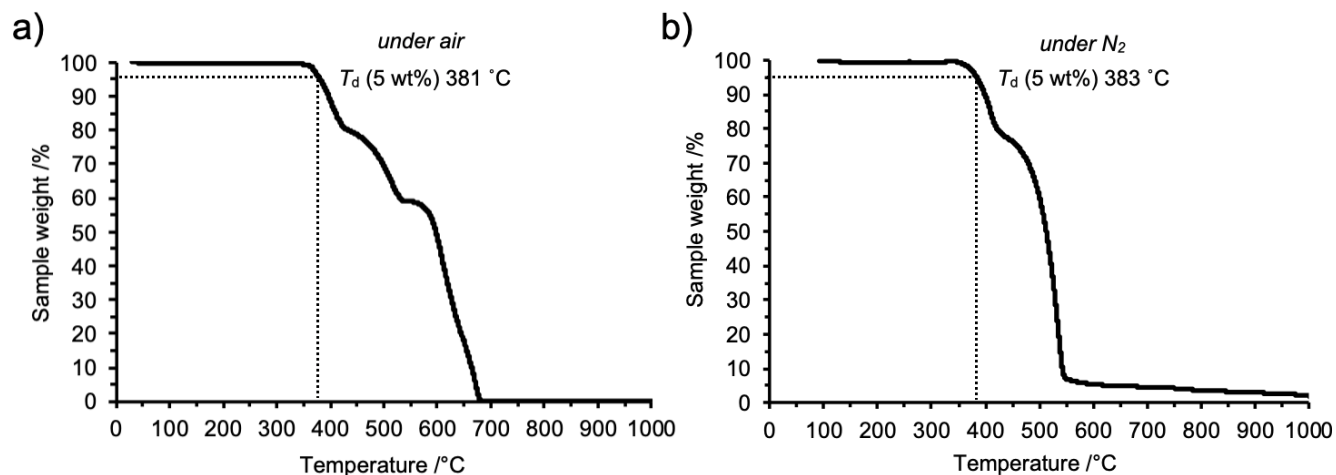


Figure S18. TGA profiles of **PSeZ-DBPHZ-PSeZ** under a) the air and b) N₂ gas flow.

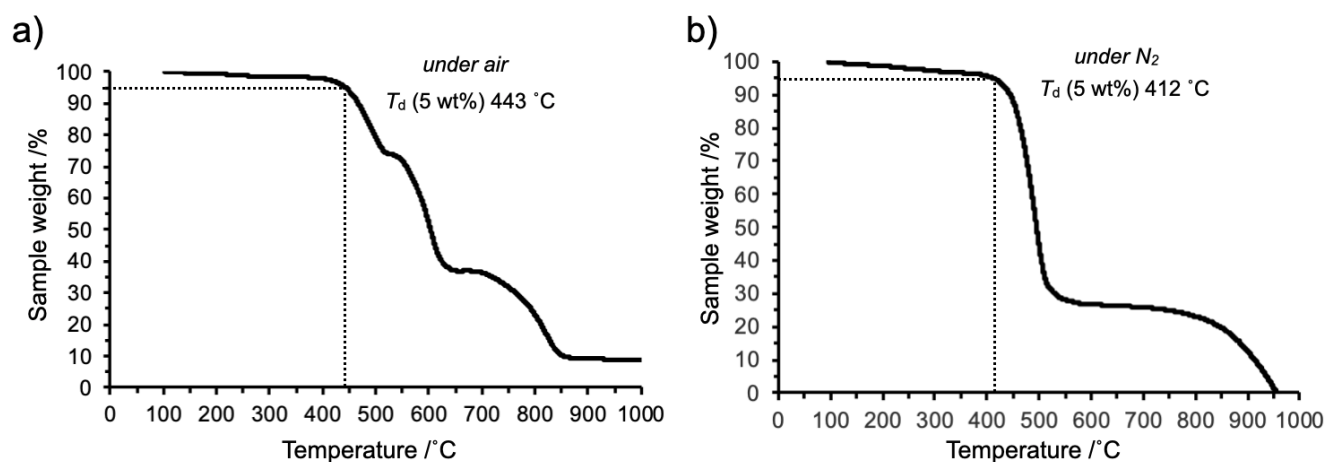
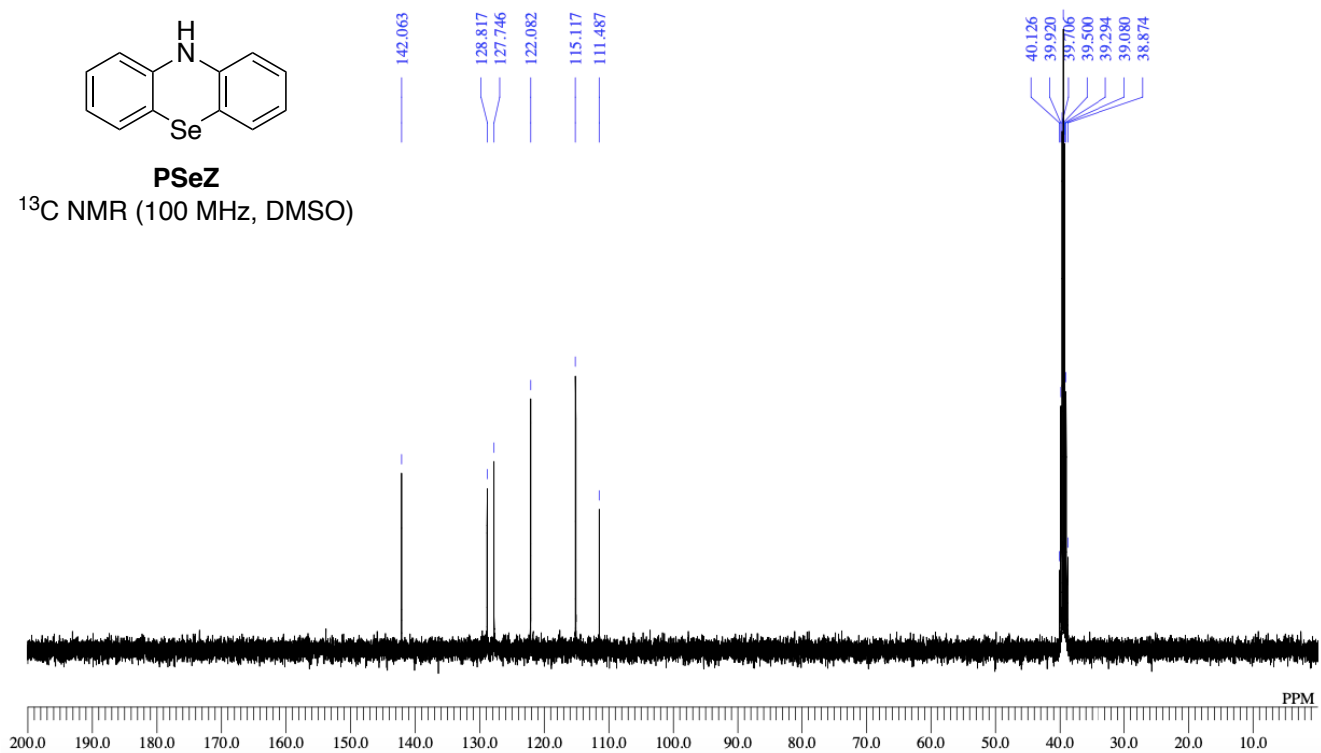
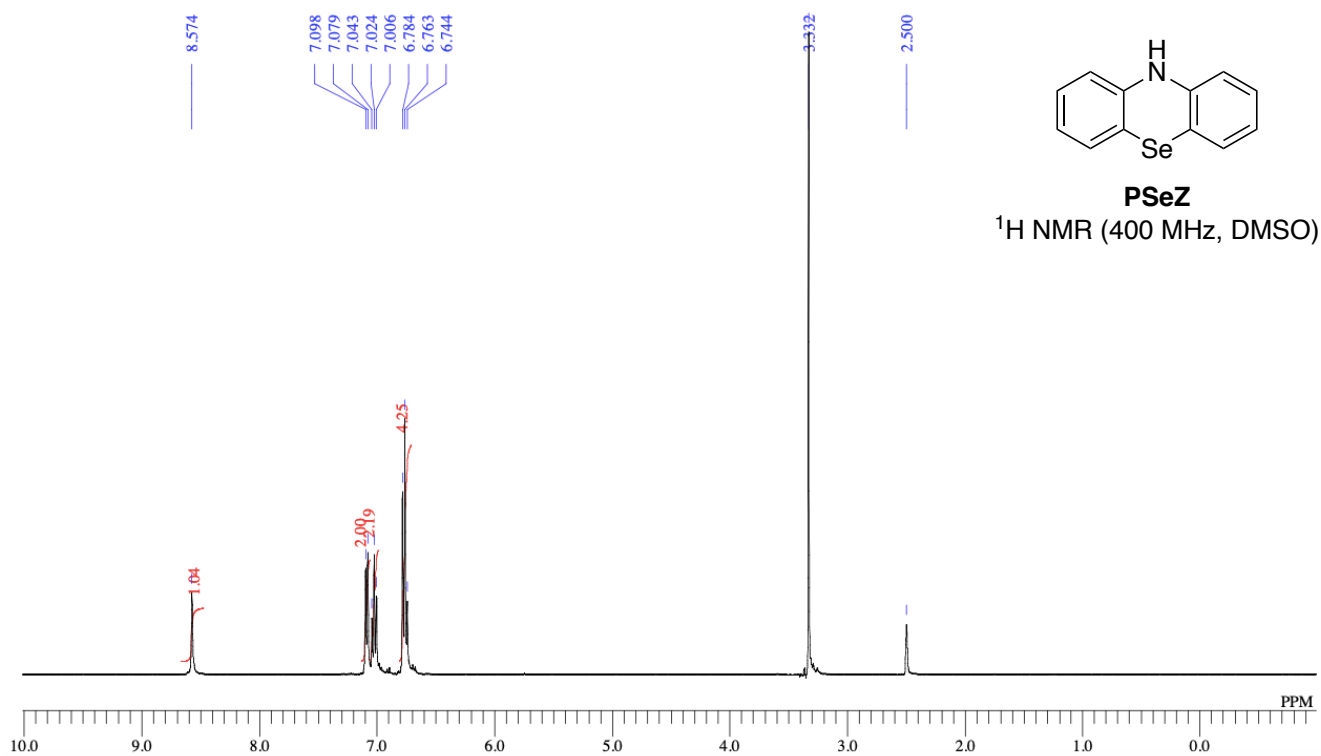


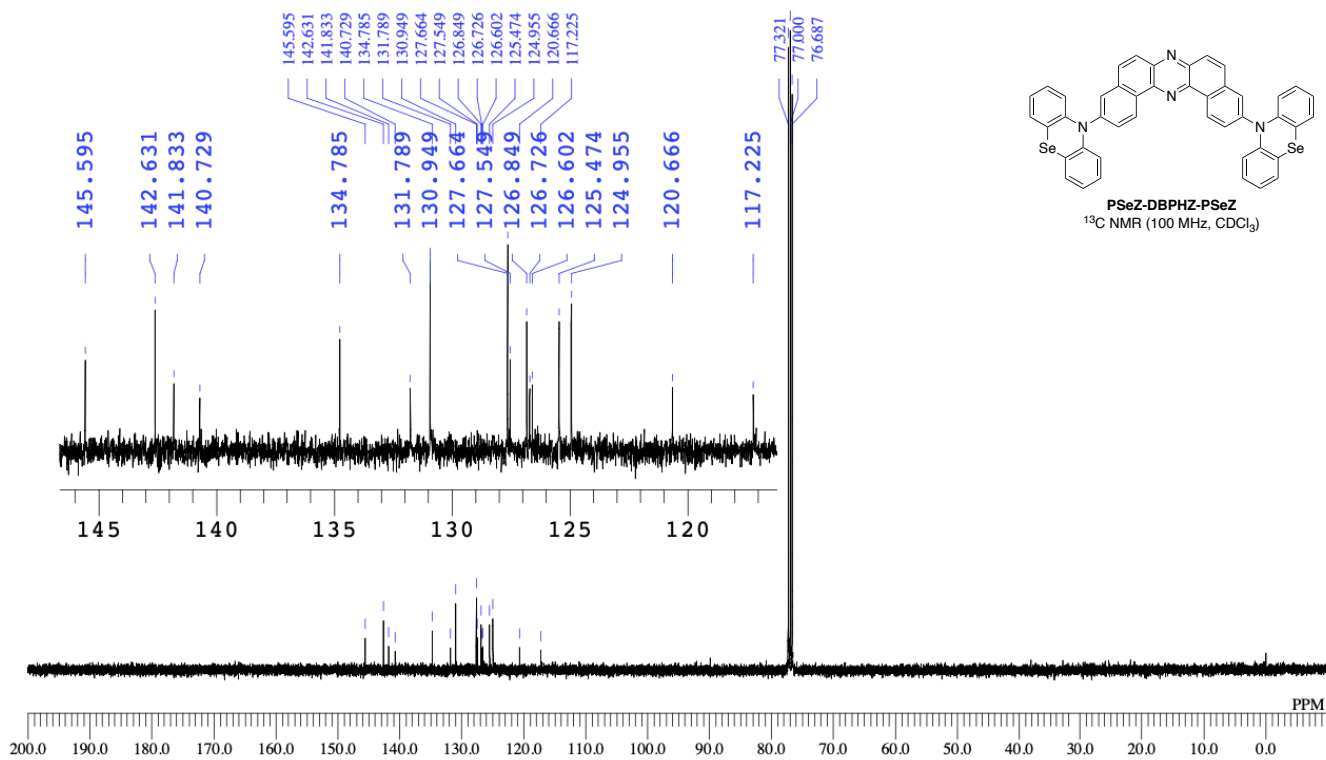
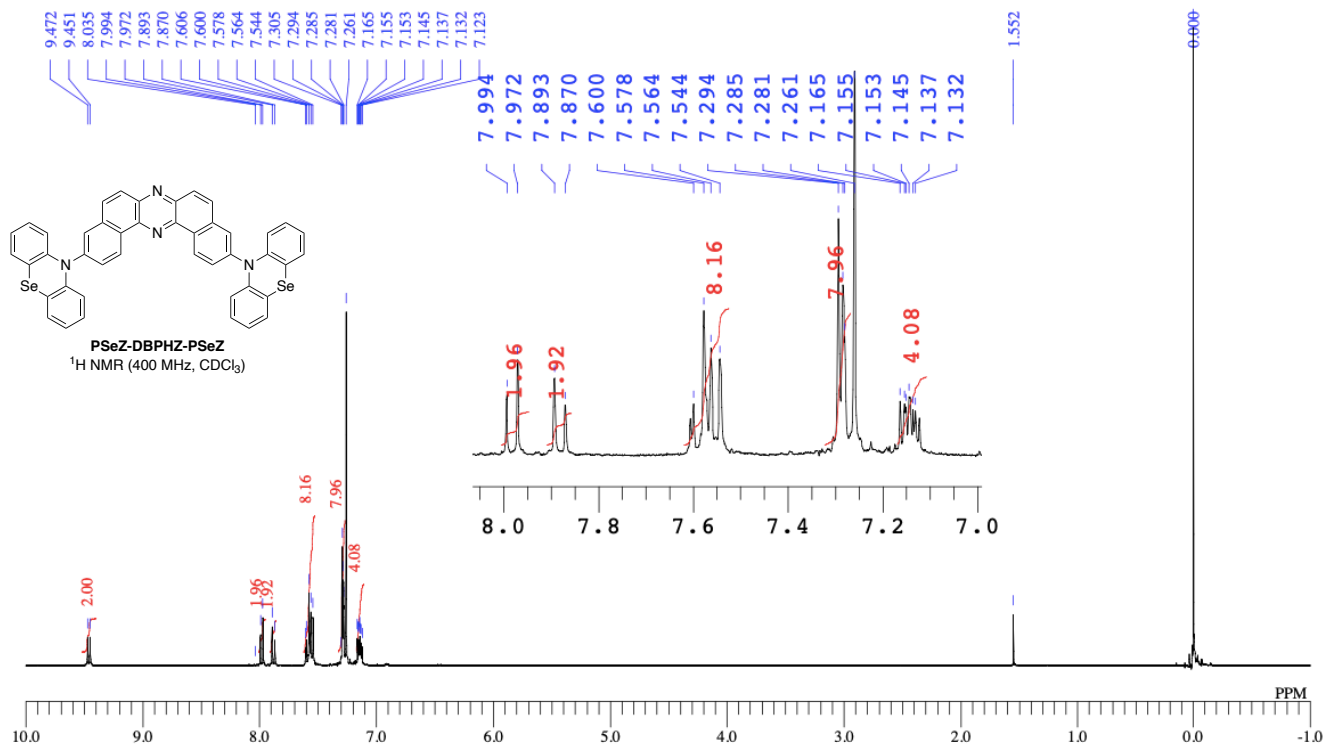
Fig. S19 TGA profiles of **PTeZ-DBPHZ-PTeZ** under a) the air and b) N₂ gas flow.

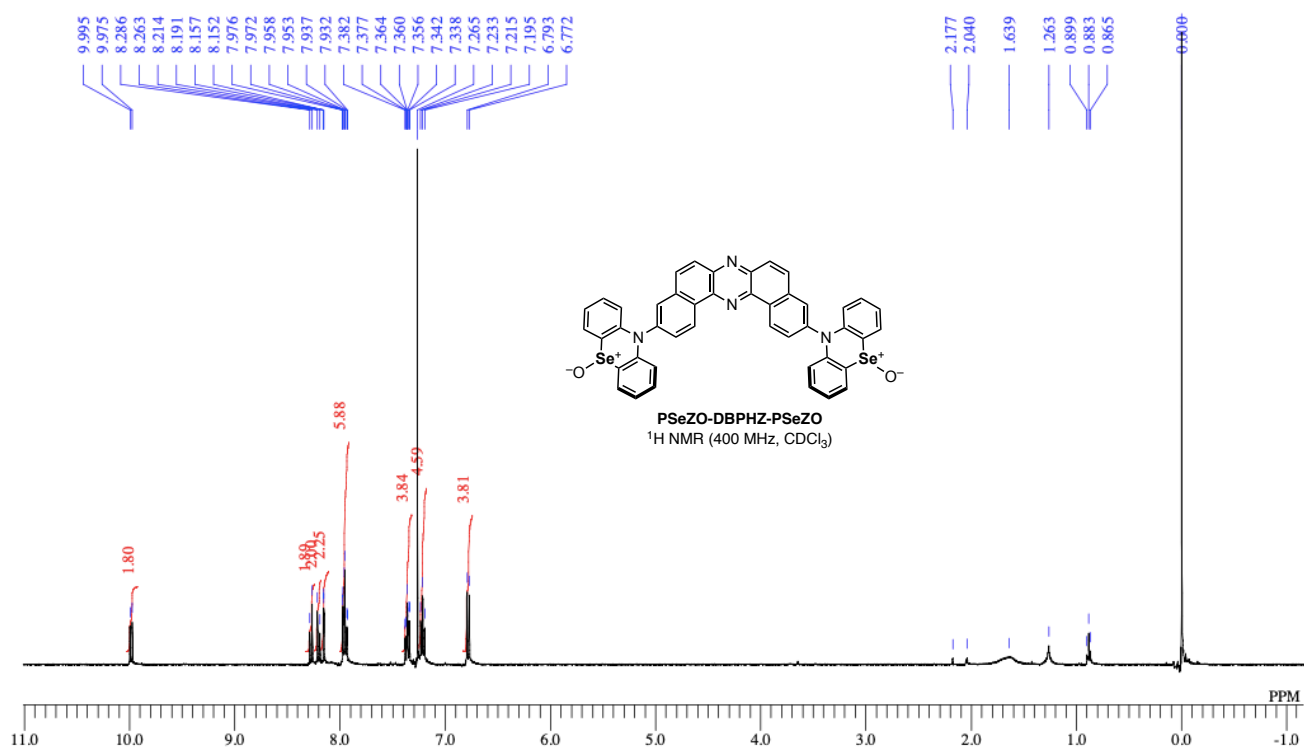
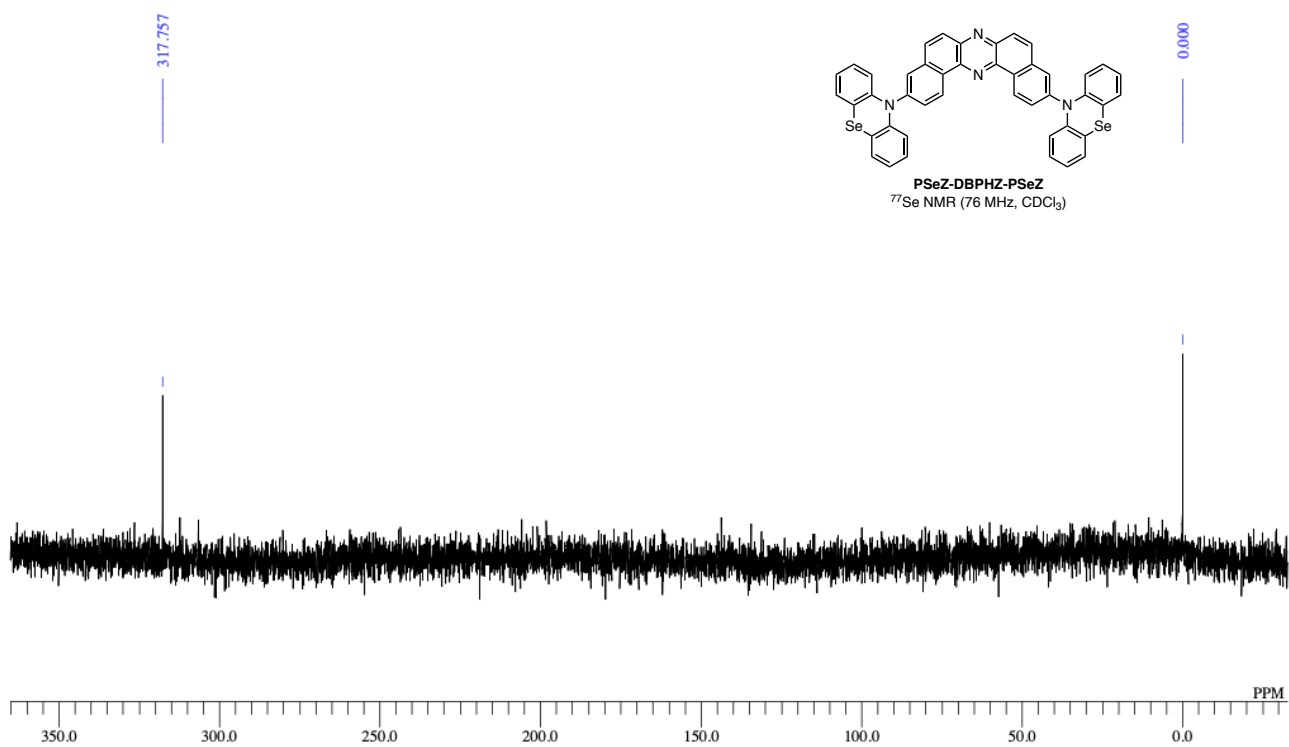
OLED Fabrication and Characterization.

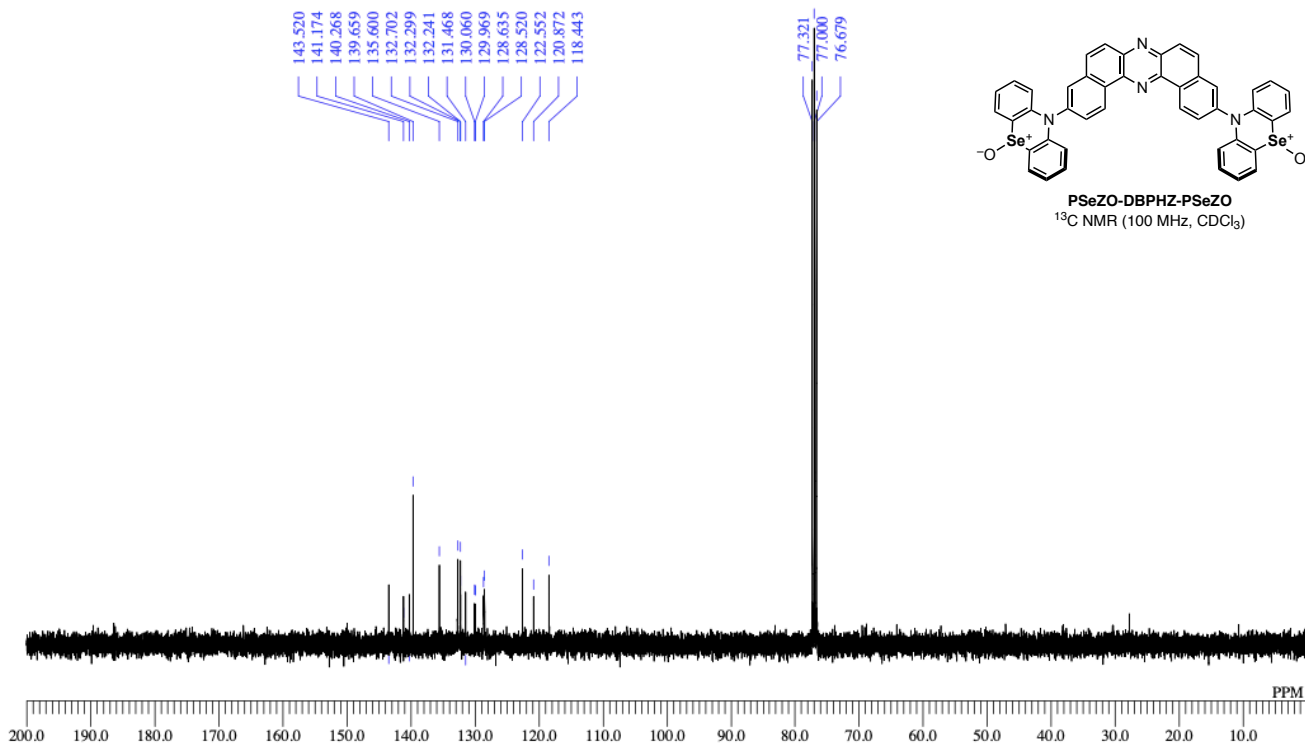
OLEDs have been fabricated on pre-cleaned, patterned indium-tin-oxide (ITO) coated glass substrates with a sheet resistance of 20 Ω /sq and ITO thickness of 100 nm. All small molecules and cathode layers were thermally evaporated in Kurt J. Lesker Spectros 150 evaporation system under pressure of 10^{-6} mbar without breaking the vacuum. The sizes of pixels were 4 mm² and 8 mm². NPB (*N,N'*-di(1-naphthyl)-*N,N'*-diphenyl-(1,1'-biphenyl)-4,4'-diamine) was used as a Hole Injection Layer (HIL) and Hole Transport Layer (HTL). CBP (4,4'-Bis(*N*-carbazolyl)-1,1'-biphenyl) was used as host and TPBi (2,2',2''-(1,3,5-Benzinetriyl)-tris(1-phenyl-1-H-benzimidazole)) as Electron Transport Layer (ETL). Lithium fluoride (LiF) and aluminium were used as the cathode. Organic semiconductors and aluminium were deposited at a rate of 1 \AA s⁻¹, and the LiF layer was deposited at 0.1 \AA s⁻¹. The characteristics of the devices were recorded using 6-inch integrating sphere (Labsphere) connected to a Source Meter Unit and Ocean Optics USB4000 spectrometer. All materials were purchased from Sigma Aldrich or Lumtec and were purified by temperature-gradient sublimation in a vacuum.

Copies of NMR Charts.

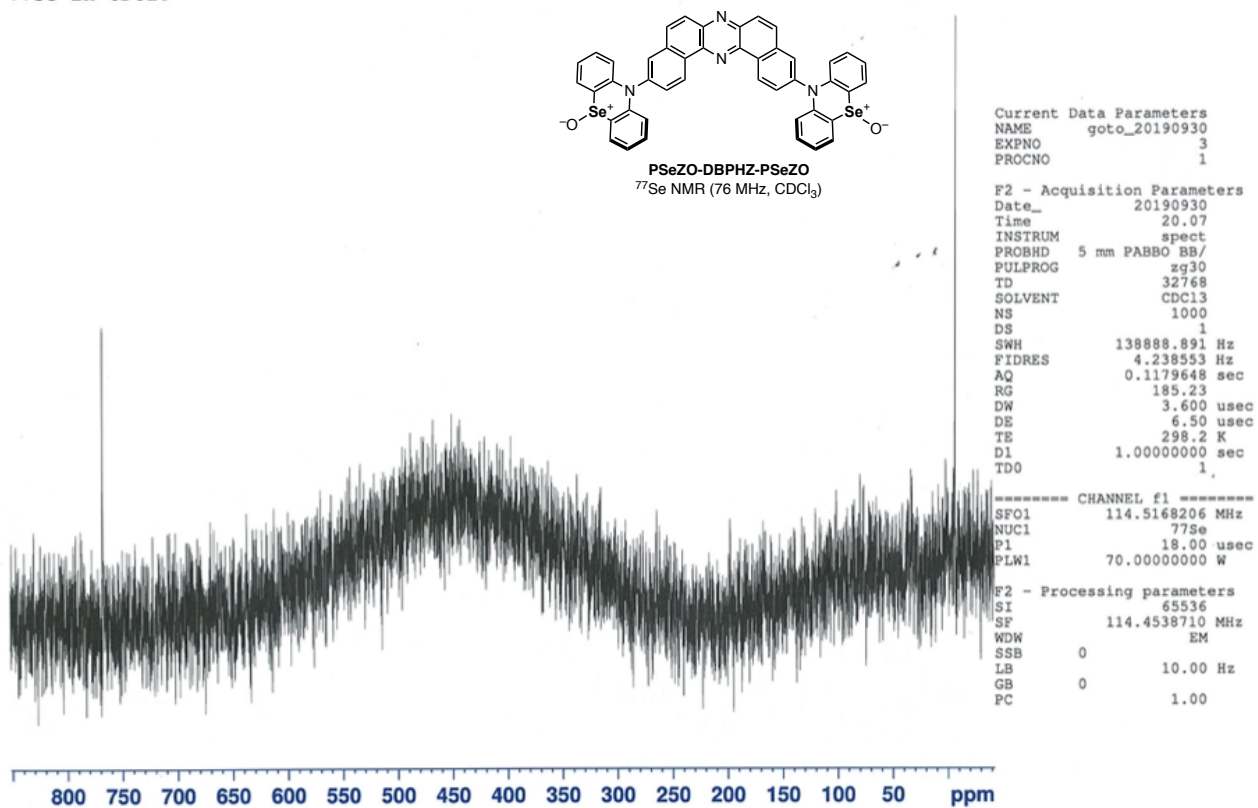


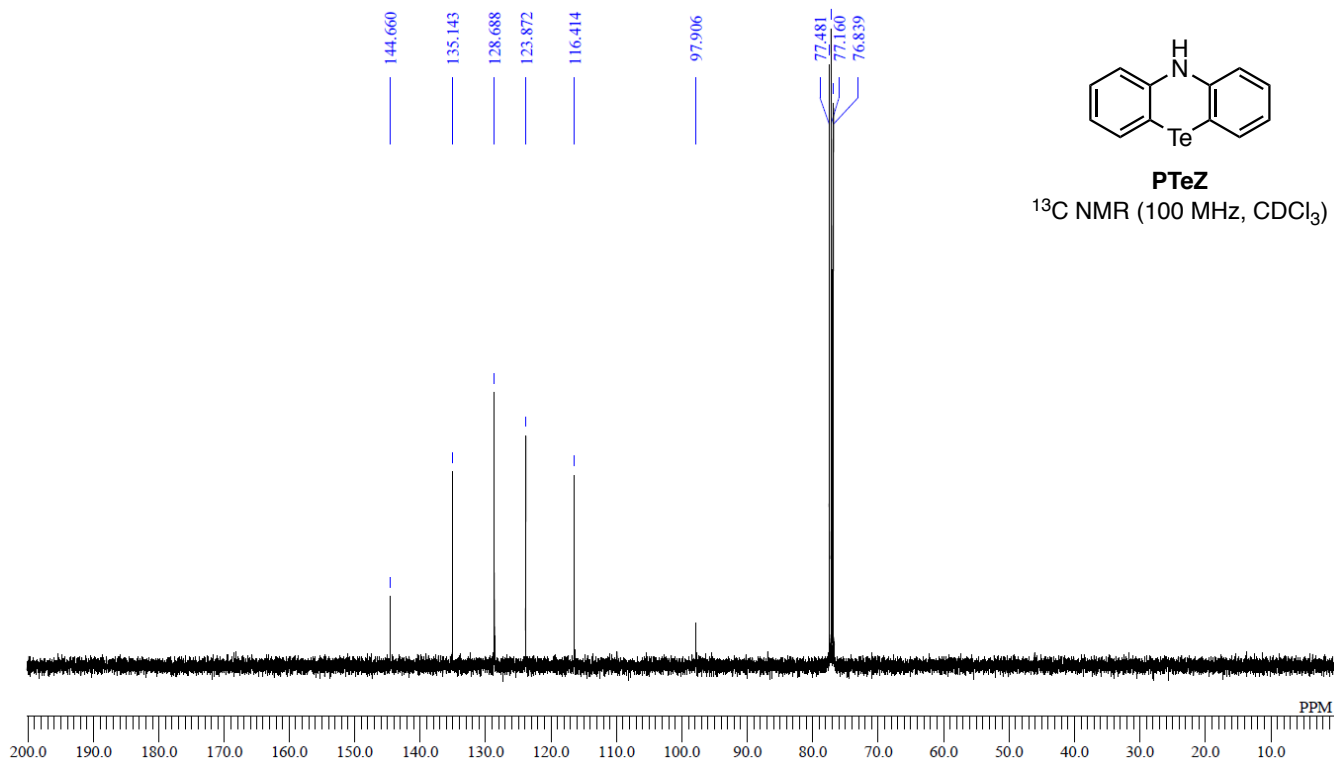
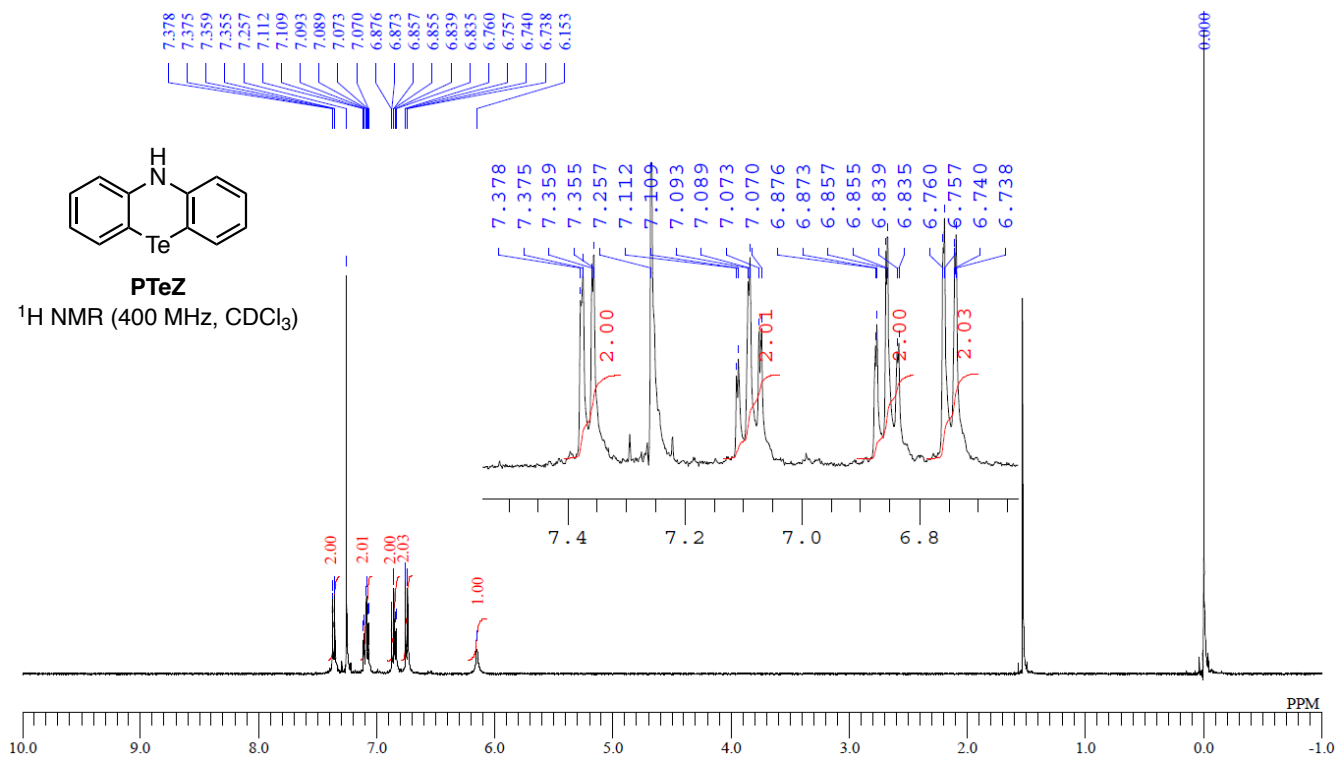


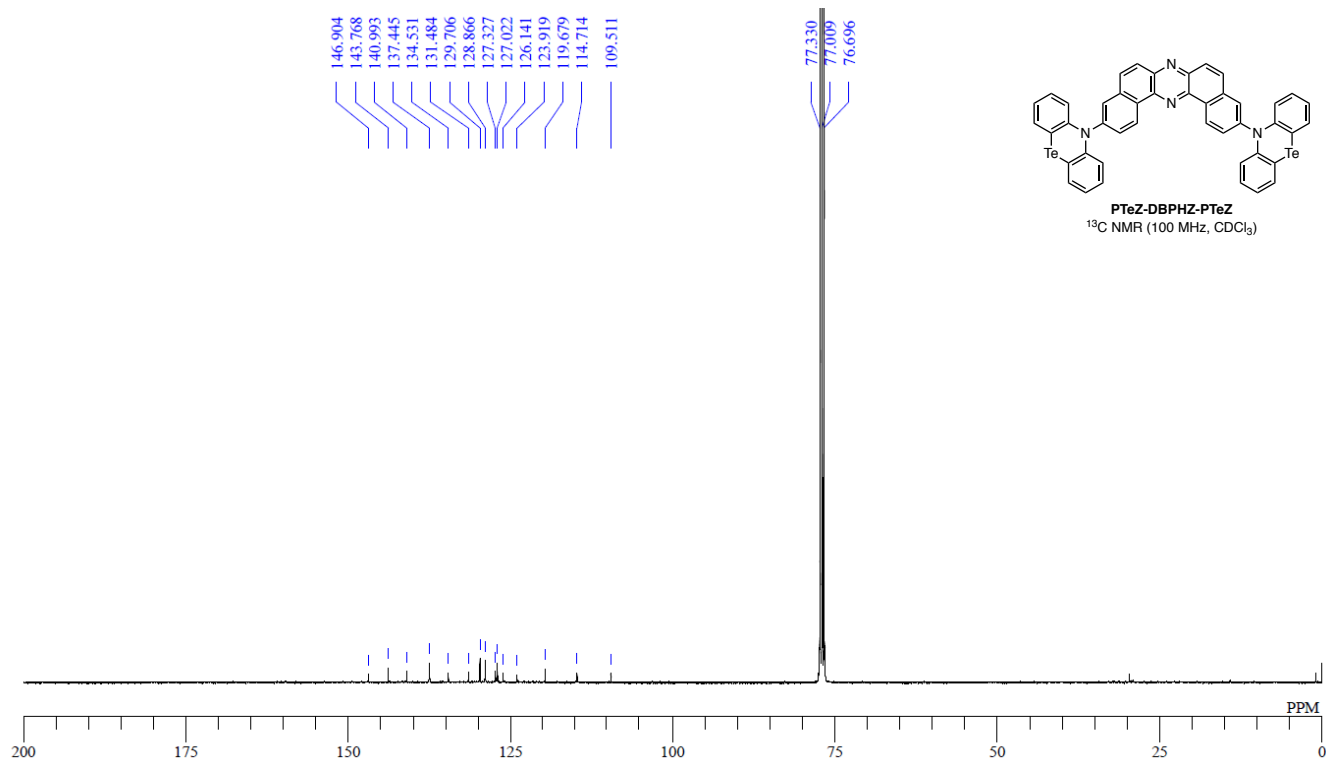
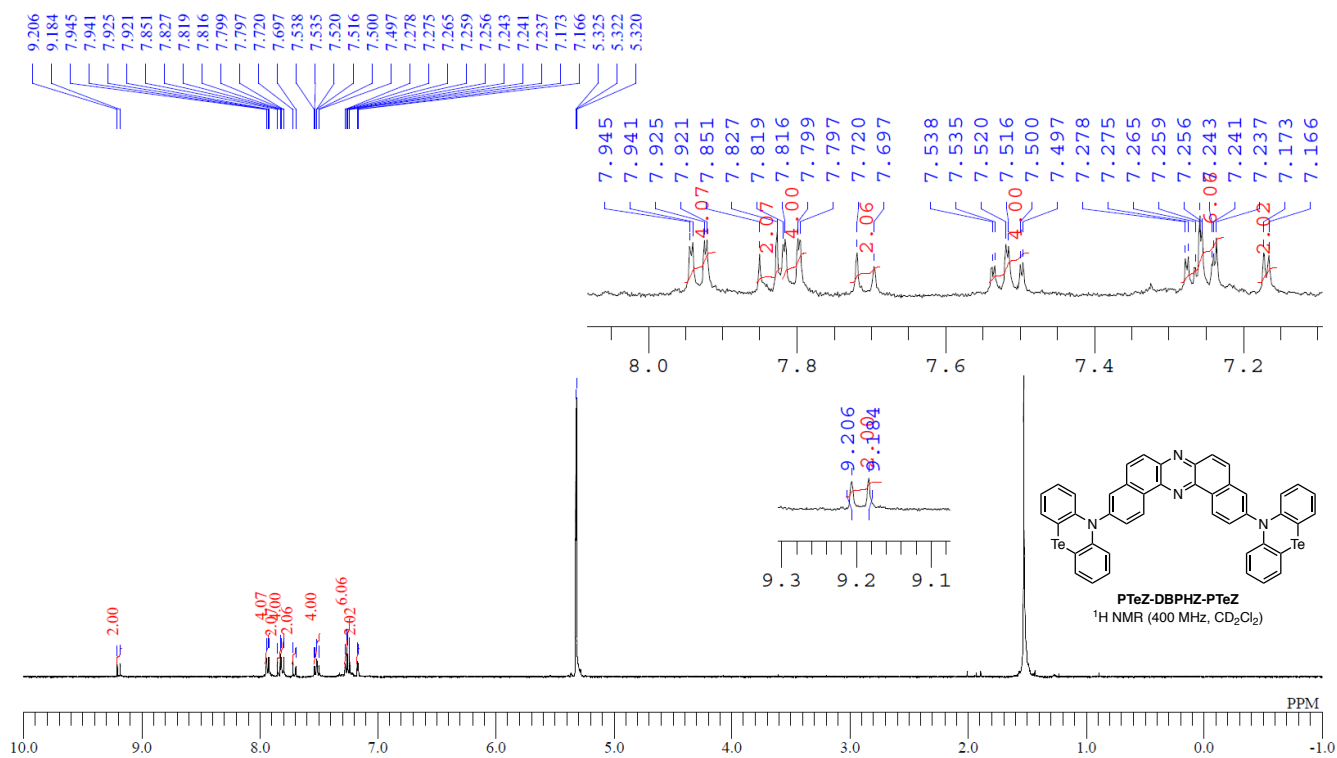


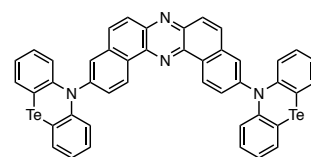


77Se in CDCl₃

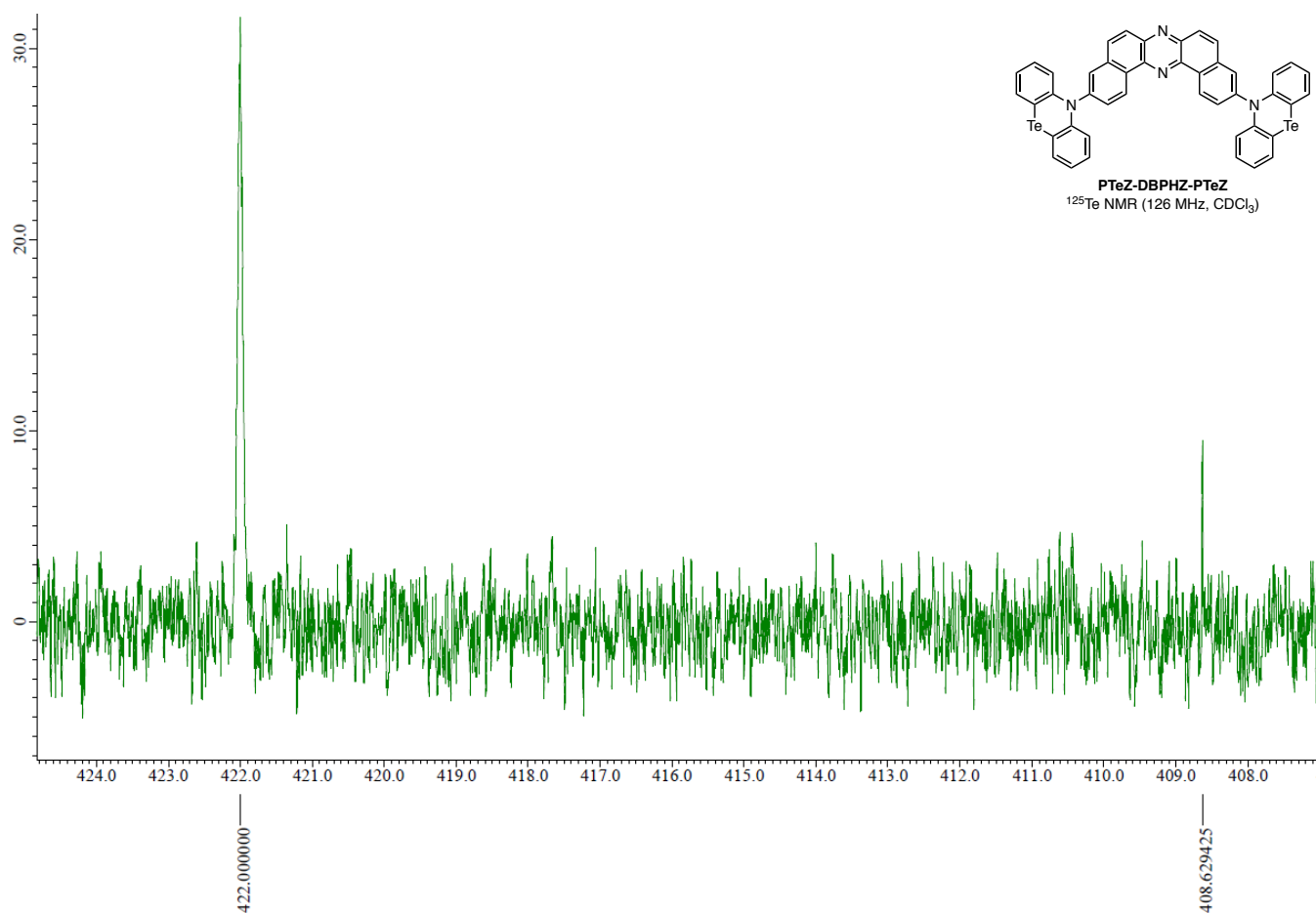








PTeZ-DBPHZ-PTeZ
¹²⁵Te NMR (126 MHz, CDCl₃)



References

- (S1) W. McFarlane and R. J. Wood, *J. Chem. Soc., Dalton Trans.*, 1972, 1397–1402.
- (S2) H. Duddeck, *Sulfur, Selenium, and Tellurium NMR*, John Wiley & Sons Ltd, Oxford, UK, 2007.
- (S3) Y. Takeda, T. Kaihara, M. Okazaki, H. Higginbotham, P. Data, N. Tohnai and S. Minakata, *Chem. Commun.*, 2018, **54**, 6847–6850.
- (S4) P. Data, P. Pander, M. Okazaki, Y. Takeda, S. Minakata and A. P. Monkman, *Angew. Chem., Int. Ed.*, 2016, **55**, 5739–5744.
- (S5) S. Hirata and M. Head-Gordon, *Chem. Phys. Lett.*, 1999, **314**, 291–299.
- (S6) Gaussian 16, Revision C.01, M. J. Frisch, G. W. Trucks, H. B. Schlegel, G. E. Scuseria, M. A. Robb, J. R. Cheeseman, G. Scalmani, V. Barone, G. A. Petersson, H. Nakatsuji, X. Li, M. Caricato, A. V. Marenich, J. Bloino, B. G. Janesko, R. Gomperts, B. Mennucci, H. P. Hratchian, J. V. Ortiz, A. F. Izmaylov, J. L. Sonnenberg, D. Williams-Young, F. Ding, F. Lipparini, F. Egidi, J. Goings, B. Peng, A. Petrone, T. Henderson, D. Ranasinghe, V. G. Zakrzewski, J. Gao, N. Rega, G. Zheng, W. Liang, M. Hada, M. Ehara, K. Toyota, R. Fukuda, J. Hasegawa, M. Ishida, T. Nakajima, Y. Honda, O. Kitao, H. Nakai, T. Vreven, K. Throssell, J. A. Montgomery, Jr., J. E. Peralta, F. Ogliaro, M. J. Bearpark, J. J. Heyd, E. N. Brothers, K. N. Kudin, V. N. Staroverov, T. A. Keith, R. Kobayashi, J. Normand, K. Raghavachari, A. P. Rendell, J. C. Burant, S. S. Iyengar, J. Tomasi, M. Cossi, J. M. Millam, M. Klene, C. Adamo, R. Cammi, J. W. Ochterski, R. L. Martin, K. Morokuma, O. Farkas, J. B. Foresman and D. J. Fox, Gaussian, Inc., Wallingford CT, 2016.
- (S7) T. Stein, L. Kronik and R. Baer, *J. Am. Chem. Soc.*, 2009, **131**, 2818–2820.
- (S8) Y. Shao, Z. Gan, E. Epifanovsky, A. T. B. Gilbert, M. Wormit, J. Kussmann, A. W. Lange, A. Behn, J. Deng, X. Feng, D. Ghosh, M. Goldey, P. R. Horn, L. D. Jacobson, I. Kaliman, R. Z. Khaliullin, T. Kúš, A. Landau, J. Liu, E. I. Proynov, Y. M. Rhee, R. M. Richard, M. A. Rohrdanz, R. P. Steele, E. J. Sundstrom, H. L. Woodcock III, P. M. Zimmerman, D. Zuev, B. Albrecht, E. Alguire, B. Austin, G. J. O. Beran, Y. A. Bernard, E. Berquist, K. Brandhorst, K. B. Bravaya, S. T. Brown, D. Casanova, C.-M. Chang, Y. Chen, S. H. Chien, K. D. Closser, D. L. Crittenden, M. Diedenhofen, R. A. DiStasio Jr., H. Dop, A. D. Dutoi, R. G. Edgar, S. Fatehi, L. Fusti-Molnar, A. Ghysels, A. Golubeva-Zadorozhnaya, J. Gomes, M. W. D. Hanson-Heine, P. H. P. Harbach, A. W. Hauser, E. G. Hohenstein, Z. C. Holden, T.-C. Jagau, H. Ji, B. Kaduk, K. Khistyayev, J. Kim, J. Kim, R. A. King, P. Klunzinger, D. Kosenkov, T. Kowalczyk, C. M. Krauter, K. U. Lao, A. Laurent, K. V. Lawler, S. V. Levchenko, C. Y. Lin, F. Liu, E. Livshits, R. C. Lochan, A. Luenser, P. Manohar, S. F. Manzer, S.-P. Mao, N. Mardirossian, A. V. Marenich, S. A. Maurer, N. J. Mayhall, C. M. Oana, R. Olivares-Amaya, D. P. O'Neill, J. A. Parkhill, T. M. Perrine, R. Peverati, P. A. Pieniazek, A. Prociuk, D. R. Rehn, E. Rosta, N. J. Russ, N. Sergueev, S. M. Sharada, S. Sharma, D. W. Small, A. Sodt, T. Stein, D. Stück, Y.-C. Su, A. J. W. Thom, T. Tsuchimochi, L. Vogt, O. Vydrov, T. Wang, M. A. Watson, J. Wenzel, A. White, C. F. Williams, V. Vanovschi, S. Yeganeh, S. R. Yost, Z.-Q. You, I. Y. Zhang, X. Zhang, Y. Zhou, B. R. Brooks, G. K. L. Chan, D. M. Chipman, C. J. Cramer, W. A. Goddard III, M. S. Gordon, W. J. Hehre, A. Klamt, H. F. Schaefer III, M. W. Schmidt, C. D. Sherrill, D. G. Truhlar, A. Warshel, X. Xua, A. Aspuru-Guzik, R. Baer, A. T. Bell, N. A. Besley, J.-D. Chai, A. Dreuw, B. D. Dunietz, T. R. Furlani, S. R. Gwaltney, C.-P. Hsu, Y. Jung, J. Kong, D. S. Lambrecht, W. Liang, C. Ochsenfeld, V. A. Rassolov, L. V. Slipchenko, J. E. Subotnik, T. Van Voorhis, J. M. Herbert, A. I. Krylov, P. M. W. Gill and M. Head-Gordon, *Molecular Phys.*, 2015, **113**, 184–215.
- (S9) M. Caricato, B. Mennucci, J. Tomasi, F. Ingrosso, R. Cammi, S. Corni and G. Scalmani, *J. Chem. Phys.*, 2006, **124**, 124520/1–13.
- (S10) (a) A. Maaninen, T. Chivers, M. Parvez, J. Pietikäinen and R. S. Laitinen, *Inorg. Chem.*, 1999, **38**, 4093–4097; (b) T. Okamoto, M. Mitani, C. P. Yu, C. Mitsui, M. Yamagishi, H. Ishii, G. Watanabe, S. Kumagai, D. Hashizume, S. Tanaka, M. Yano, T. Kushida, H. Sato, K. Sugimoto, T. Kato and J. Takeya, *J. Am. Chem. Soc.*, 2020, **142**, 14974–14984.
- (S11) G. Tin, T. Mohamed, N. Gondora, M. A. Beazely and P. P. N. Rao, *Med. Chem. Commun.*, 2015, **6**, 1930–1941.
- (S12) T. Junk and J. K. Irgolic, *Heterocycles*, 1989, **28**, 1007–1013.
- (S13) C. Weilbeer, D. Selent, K. M. Dyballa, R. Franke, A. Spannenberg and A. Börner, *ChemistrySelect*, 2016, **1**, 5421–5429.
- (S14) A. M. Toma, A. Nicoară, A. Silvestru, T. Ruffer, H. Lang and M. Mehring, *J. Organomet. Chem.*, 2016, **810**, 33–39.
- (S15) Rigaku Oxford Diffraction (2015), Software CrysAlisPro 1.171.39.5a Rigaku Corporation, Tokyo, Japan.
- (S16) SHELXT Version 2014/5. G. M. Sheldrick, *Acta Cryst.*, 2014, **A70**, C1437.

- (S17) CrystalStructure 4.3: Crystal Structure Analysis Package, Rigaku Corporation (2000-2018). Tokyo 196-8666, Japan.
- (S18) SHELXL Version 2018/1: G. M. Sheldrick, *Acta Cryst.*, 2008, **A64**, 112–122.
- (S19) (a) C. M. Cardona, W. Li, A. E. Kaifer, D. Stockdale and G. C. Bazan, *Adv. Mater.*, 2011, **23**, 2367–2371;
(b) J.-L. Bredas, *Mater. Horiz.*, 2014, **1**, 17–19.